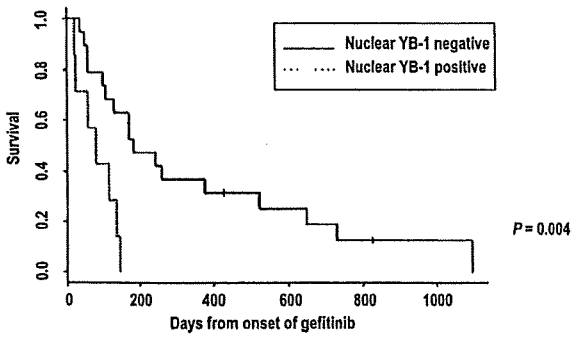

FIGURE 5. Kaplan-Meier estimate for time to further progressive disease from the initiation of gefitinib according to nuclear YB-1 expression in 26 patients treated with gefitinib after progressive disease.

unknown. Immunohistochemical analysis of clinical samples of NSCLC showed that nuclear YB-1 expression was negatively correlated with HER3 expression in squamous cell carcinoma ($p = 0.038$) and positively correlated with HER2 expression in adenocarcinoma ($p = 0.052$). However, nuclear YB-1 expression was not significantly correlated with EGFR or c-Met expression in either squamous cell carcinoma or adenocarcinoma.

Overexpression of HER2 in an NSCLC cell line with very low EGFR and high HER3 expression levels sensitizes these cells to growth inhibition by the EGFR-targeting drug gefitinib, and gefitinib abrogated formation of HER2/HER3 heterodimers.[24] Consistent with this report, there is a strong correlation between HER3 expression and sensitivity to gefitinib.[25] Another EGFR-targeting drug, erlotinib, also inhibits HER2 tyrosine kinase, and HER2/HER3 heterodimer formation sensitizes lung cancer cells to growth inhibition by erlotinib.[26] Taken together, expression of HER2 and HER3 coupled with formation of their heterodimers plays a critical role in determining the therapeutic efficacy of the EGFR-targeting drugs gefitinib and erlotinib.[27,28] The possible link between nuclear YB-1 expression and HER2 expression in adenocarcinoma ($p = 0.052$) might be in part responsible for the correlation between nuclear YB-1 expression and survival of patients with adenocarcinoma NSCLC. Nuclear YB-1 expression is positively correlated with HER2 expression in patients with breast cancer ($p = 0.015$).[9] Thus, HER2 expression could be modulated by nuclear YB-1 expression not only in patients with breast cancer[9] but also in patients with adenocarcinoma NSCLC (this study). HER3 expression was inversely correlated with nuclear expression of YB-1 in squamous cell carcinoma ($p = 0.038$), but HER3 expression alone did not correlate with survival of patients with NSCLC or of the subset with squamous cell carcinoma. It seems unlikely that the inverse correlation of nuclear YB-1 expression with HER3 expression is a factor in the poor prognosis associated with nuclear YB-1 expression in patients with squamous NSCLC.

In addition to the effect of altering the status of EGFR family proteins on the therapeutic efficacy of EGFR-targeting drugs, amplification of c-Met has been identified as another acquired drug resistance mechanism.[29] c-Met modifies drug sensitivity to gefitinib through HER3-dependent activation of the PI3K/Akt pathway.[25] Moreover, Cappuzzo et al.[30] reported that gefitinib-treated patients with a high-HER3 gene copy number had significantly higher response rates and times to progression, although with no improvement in overall survival. Nuclear expression of YB-1 also affected expression of c-Met in two NSCLC cell lines in culture, but we could not observe any significant correlation between nuclear YB-1 expression and c-Met expression in NSCLC. This suggests that it is unlikely that nuclear YB-1 expression determines c-Met expression in patients with NSCLC.

Nuclear YB-1 expression is often associated with poor prognosis in various human malignancies, including breast cancer.[4–10] In NSCLC, our previous IHC study on 196 patients demonstrated that nuclear YB-1 expression is significantly associated with poor prognosis in all patients ($p = 0.0424$) and in patients with squamous cell carcinoma ($p = 0.0313$), but not in patients with adenocarcinoma ($p = 0.2015$).[8] This study demonstrated a close association of nuclear YB-1 expression with poor prognosis in all patients ($p = 0.028$) and in patients with adenocarcinoma ($p = 0.007$), but not in patients with squamous cell carcinoma ($p = 0.381$). This inconsistency may result from the small number of patients with squamous cell carcinoma in this study. The results of the Cox regression analysis given in Table 3 provide similar estimates of the HR of nuclear YB-1 expression in adenocarcinoma and squamous cell carcinoma, although they were not necessarily statistically significant. Further studies with more definitive clinicopathological characterization of the patients included are required to establish the types of NSCLC in which nuclear expression of YB-1 predicts poor prognosis.

Of patients with NSCLC ($n = 104$) tested in this study, we examined whether therapeutic efficacies of gefitinib were associated with expression levels of nuclear YB-1 expression when recurrent 26 patients (24 adenocarcinoma and two squamous cell carcinoma) were treated with gefitinib. Although the number of treated patients was small, the absence or presence of nuclear YB-1 expression shows a significant correlation with differences in the survival curves after progression disease. Concerning EGFR mutations that are highly susceptible to the therapeutic efficacy of gefitinib, we also observed statistically significant differences between patients with mutant EGFR and those with wild-type EGFR (Azuma et al, unpublished data). Nuclear YB-1 expression might have a significant predictive value for progression disease in patients with NSCLC when treated with EGFR-targeting drug. Further study is in progress whether nuclear expression of YB- 49 could be associated with gefitinib-susceptible EGFR mutations.

In conclusion, our results show that nuclear YB-1 expression is strongly associated with overall survival of patients with NSCLC ($n = 104$). Of the EGFR family proteins, nuclear YB-1 expression is associated with expression of HER2 in both histologic types of NSCLC and of HER3 in squamous cell carcinoma type of NSCLC. Therefore, expression of YB-1 in the nucleus might affect the therapeutic efficacy of EGFR-targeting drugs. Nuclear YB-1

expression is associated with progressive disease survival of patients with NSCLC ($n = 26$) when treated with gefitinib. Together, these observations indicate that nuclear YB-1 is a novel biomarker in NSCLC.

ACKNOWLEDGMENTS

Supported by a grant-in-aid for Scientific Research on Priority Areas, Cancer, from the Ministry of Education, Culture, Sports, Science and Technology of Japan (to M.O.), and by the 3rd Term Comprehensive Control Research for Cancer from the Ministry of Health, Labor and Welfare, Japan (to M.K.). Also supported, in part, by the Formation of Innovation Center for Fusion of Advanced Technologies, Kyushu University, Japan (to M.O., Y.B., and M.K.).

The authors thank Kimitoshi Kohno and Hiroto Izumi (University of Occupational and Environmental Health) for their fruitful discussion.

REFERENCES

1. Matsumoto K, Wolffe AP. Gene regulation by Y-box proteins: coupling control of transcription and translation. *Trends Cell Biol* 1998;8:318–323.
2. Kohno K, Izumi H, Uchiumi T, Ashizuka M, Kuwano M. The pleiotropic functions of the Y-box-binding protein, YB-1. *Bioessays* 2003;25:691–698.
3. Kuwano M, Oda Y, Izumi H, et al. The role of nuclear Y-box binding protein 1 as a global marker in drug resistance. *Mol Cancer Ther* 2004;3:1485–1492.
4. Kamura T, Yahata H, Amada S, et al. Is nuclear expression of Y-box binding protein-1 a new prognostic factor in ovarian serous adenocarcinoma? *Cancer* 1999;85:2450–2454.
5. Oda Y, Ohishi Y, Basaki Y, et al. Prognostic implication of the nuclear localization of the Y-box binding protein-1 and CXCR4 expression in ovarian cancer: their correlation with activated Akt, LRP/MVP and *P*-glycoprotein expression. *Cancer Sci* 2007;98:1020–1026.
6. Ladomery M, Sommerville J. A role for Y-box proteins in cell proliferation. *Bioessays* 1995;17:9–11.
7. Oda Y, Kohashi K, Yamamoto H, et al. Different expression profiles of Y-box-binding protein-1 and multidrug resistance-associated proteins between alveolar and embryonal rhabdomyosarcoma. *Cancer Sci* 2008;99:726–732.
8. Shibahara K, Sugio K, Osaki T, et al. Nuclear expression of the Y-box binding protein as a novel marker of disease progression in non-small cell lung cancer. *Clin Cancer Res* 2001;7:3151–3155.
9. Fujii T, Kawahara A, Basaki Y, et al. Expression of HER2 and estrogen receptor alpha depends upon nuclear localization of Y-box binding protein-1 in human breast cancers. *Cancer Res* 2008;68:1504–1512.
10. Faury D, Nantel A, Dunn SE, et al. Molecular profiling identifies prognostic subgroups of pediatric glioblastoma and shows increased YB-1 expression in tumors. *J Clin Oncol* 2007;25:1196–1208.
11. Sutherland BW, Kucab J, Wu J, et al. Akt phosphorylates the Y-box binding protein 1 at Ser 102 located in the cold shock domain and affects the anchorage-independent growth of breast cancer cells. *Oncogene* 2005;24:4281–4292.
12. Basaki Y, Hosoi F, Oda Y, et al. Akt-dependent nuclear localization of Y-box binding protein 1 in acquisition of malignant characteristics by human ovarian cancer cells. *Oncogene* 2007;26:2736–2746.
13. Jurchott K, Bergmann S, Stein U, et al. YB-1 as a cell cycle-regulated transcription factor facilitating cyclin A and B1 gene expression. *J Biol Chem* 2003;278:27988–27996.
14. Bergmann S, Royer-Pokara B, Fietze E, et al. YB-1 provokes breast cancer through the induction of chromosomal instability that emerges from mitotic failure and centrosome amplification. *Cancer Res* 2005;65:4078–4087.
15. Lu ZH, Books JT, Ley TJ. YB-1 is important for late-stage embryonic development, optimal cellular stress responses, and the prevention of premature senescence. *Mol Cell Biol* 2005;25:4625–4637.
16. Uchiumi T, Fotovati A, Sasaguri T, et al. YB-1 is important for an early stage embryonic development: neural tube formation and cell proliferation. *J Biol Chem* 2006;281:40440–40449.
17. Berquin IM, Pang B, Dziubinski ML, et al. Y-box-binding protein 1 confers EGF independence to human mammary epithelial cells. *Oncogene* 2005;24:3177–3186.
18. Wu J, Lee C, Yokom D, et al. Disruption of the Y-box binding protein-1 results in suppression of the epidermal growth factor receptor and HER-2. *Cancer Res* 2006;66:4872–4879.
19. Janz M, Harbeck N, Dettmar P, et al. Y-box factor YB-1 predicts drug resistance and patient outcome in breast cancer independent of clinically relevant tumor biologic factors HER2, uPA and PAI-1. *Int J Cancer* 2002;97:278–282.
20. Stratford AL, Habibi G, Astanehe A, et al. Epidermal growth factor receptor (EGFR) is transcriptionally induced by the Y-box binding protein-1 (YB-1) and can be inhibited with Iressa in basal-like breast cancer, providing a potential target for therapy. *Breast Cancer Res* 2007;9:R61.
21. Ohga T, Koike K, Ono M, et al. Role of the human Y box-binding protein YB-1 in cellular sensitivity to the DNA-damaging agents cisplatin, mitomycin C, and ultraviolet light. *Cancer Res* 1996;56:4224–4228.
22. Simpson EH. The interpretation of interaction in contingency table. *J R Stat Soc B* 1951;13:238–241.
23. Rothman KJ, Greenland S. (1998) Modern Epidemiology, 2nd Ed. Philadelphia: Lippincott-Raven, 1998. P. 113.
24. Hirata A, Hosoi F, Miyagawa M, et al. HER2 overexpression increases sensitivity to gefitinib, an epidermal growth factor receptor tyrosine kinase inhibitor, through inhibition of HER2/HER3 heterodimer formation in lung cancer cells. *Cancer Res* 2005;65:4253–4260.
25. Engelman JA, Jänne PA. Mechanisms of acquired resistance to epidermal growth factor receptor tyrosine kinase inhibitors in non-small cell lung cancer. *Clin Cancer Res* 2008;14:2895–2899.
26. Schaefer G, Shao L, Totpal K, Akita RW. Erlotinib directly inhibits HER2 kinase activation and downstream signaling events in intact cells lacking epidermal growth factor receptor expression. *Cancer Res* 2007;67:1228–1238.
27. Ono M, Kuwano M. Molecular mechanisms of epidermal growth factor receptor (EGFR) activation and response to gefitinib and other EGFR-targeting drugs. *Clin Cancer Res* 2006;12:7242–7251.
28. Reinmuth N, Meister M, Muley T, et al. Molecular determinants of response to RTK-targeting agents in nonsmall cell lung cancer. *Int J Cancer* 2006;119:727–734.
29. Engelman JA. The role of phosphoinositide 3-kinase pathway inhibitors in the treatment of lung cancer. *Clin Cancer Res* 2007;13:4637–4640.
30. Cappuzzo F, Toschi L, Domenichini I, et al. HER3 genomic gain and sensitivity to gefitinib in advanced non-small-cell lung cancer patients. *Br J Cancer* 2005;93:1334–1340.

N-myc Downstream Regulated Gene 1/Cap43 Suppresses Tumor Growth and Angiogenesis of Pancreatic Cancer through Attenuation of Inhibitor of κB Kinase β Expression

Fumihito Hosoi,[1,3] Hiroto Izumi,[6] Akihiko Kawahara,[3,4] Yuichi Murakami,[1] Hisafumi Kinoshita,[5] Masayoshi Kage,[3,4] Kazuto Nishio,[7] Kimitoshi Kohno,[6] Michihiko Kuwano,[2] and Mayumi Ono[1]

[1]Department of Pharmaceutical Oncology, Graduate School of Pharmaceutical Sciences and [2]Innovation Center for Medical Redox Navigation, Kyushu University, Fukuoka, Japan; [3]Research Center for Innovative Cancer Therapy, Kurume University; [4]Department of Pathology, Kurume University Hospital; [5]Department of Surgery, Kurume University School of Medicine, Kurume, Japan; [6]Department of Molecular Biology, University of Occupational and Environmental Health, Kitakyushu, Japan; and [7]Department of Genome Biology, Kinki University School of Medicine, Osaka, Japan

Abstract

N-myc downstream regulated gene 1 (NDRG1)/Cap43 expression is a predictive marker of good prognosis in patients with pancreatic cancer as we reported previously. In this study, NDRG1/Cap43 decreased the expression of various chemoattractants, including CXC chemokines for inflammatory cells, and the recruitment of macrophages and neutrophils with suppression of both angiogenesis and growth in mouse xenograft models. We further found that NDRG1/Cap43 induced nuclear factor-κB (NF-κB) signaling attenuation through marked decreases in inhibitor of κB kinase (IKK) β expression and IκBα phosphorylation. Decreased IKKβ expression in cells overexpressing NDRG1/Cap43 resulted in reduction of both nuclear translocation of p65 and p50 and their binding to the NF-κB motif. The introduction of an exogenous IKKβ gene restored NDRG1/Cap43-suppressed expression of melanoma growth-stimulating activity α/CXCL1, epithelial-derived neutrophil activating protein-78/CXCL5, interleukin-8/CXCL8 and vascular endothelial growth factor-A, accompanied by increased phosphorylation of IκBα in NDRG1/Cap43-expressing cells. In patients with pancreatic cancer, NDRG1/Cap43 expression levels were also inversely correlated with the number of infiltrating macrophages in the tumor stroma. This study suggests a novel mechanism by which NDRG1/Cap43 modulates tumor angiogenesis/growth and infiltration of macrophages/neutrophils through attenuation of NF-κB signaling. [Cancer Res 2009;69(12):4983–91]

Introduction

N-myc downstream regulated gene 1 (NDRG1)/Cap43 is one of the metastasis suppressor genes (1), and expression of NDRG1/Cap43 is regulated by oncogenes (*N-myc* and *C-myc*) and tumor suppressor genes (*p53, VHL,* and *PTEN*; ref. 2). Expression of NDRG1/Cap43 protein is often elevated in many types of human tumors. In human cancer, expression of NDRG1/Cap43 depends on tumor type and differentiation status (2). Consistent with this idea, NDRG1/Cap43 expression in cancer cells is a predictive marker of good prognosis in patients with neuroblastoma or cancers of the prostate, breast, esophagus, colon, and pancreas (3–10), whereas its expression is a predictive marker of poor prognosis in patients with liver and cervical cancer (11, 12).

We previously identified *NDRG1/Cap43* as one of the nine genes that are highly expressed in cancerous regions of human renal cell carcinoma (13), and its expression is closely associated with the *VHL* oncosuppressor gene (14). We further showed that expression of NDRG1/Cap43 is associated with a marked decrease of tumor angiogenesis in mice bearing human pancreatic cancer xenografts and that NDRG1/Cap43 markedly suppresses the expression of matrix metalloproteinase-9, vascular endothelial growth factor (VEGF), and interleukin (IL)-8/CXCL8. Moreover, expression of NDRG1/Cap43 has been associated with decreased microvessel density (MVD) and differentiation or depth of invasion in cancer cells in patients with pancreatic cancer (5).

In the present study, we further examined how NDRG1/Cap43 modulates tumor growth and angiogenesis in pancreatic cancer. Because microarray analysis in this study and our previous studies showed that expression of some angiogenesis- and inflammation-related factors were markedly down-regulated by NDRG1/Cap43, we hypothesized that inflammation could be somehow associated with the NDRG1/Cap43-induced suppression of tumor growth and angiogenesis. Our results indicated that down-regulation of CXC chemokines and VEGF expression by NDRG1/Cap43 was actively involved in its suppression of angiogenesis and growth in pancreatic cancer as well as infiltration of macrophages and neutrophils, and we discuss whether attenuation of nuclear factor-κB (NF-κB) signaling plays a key role in this process.

Materials and Methods

Materials and cell lines. MIApaca-2 transfectants (Mock#2, Cap#11 and Cap#14) were maintained in DMEM supplemented with 10% fetal bovine serum and G418. The anti-NDRG1/Cap43 antibody was generated as described previously (5). Other antibodies were purchased as follows: anti-β-actin antibody (Abcam); anti-NIK, anti-TAB1/2, anti-TAK1, anti-inhibitor of κB kinase (IKK) α, anti-IKKβ, anti-IKKγ, anti-p-IκBα, anti-p65, anti-p50, anti-RelB, anti-p52, and anti-ubiquitin antibodies (Cell Signaling Technology); anti-p65 and anti-p50 antibodies for supershift analysis by electromobility shift assay (EMSA; Santa Cruz Biotechnology); anti-Flag M2 antibody (Sigma); and anti-CD68 and anti-neutrophil elastase antibodies (DAKO). Human tumor necrosis factor-α (TNF-α) and MG-132 was purchased from R&D Systems and Calbiochem.

Note: Supplementary data for this article are available at Cancer Research Online (http://cancerres.aacrjournals.org/).

Requests for reprints: Mayumi Ono, Department of Pharmaceutical Oncology, Graduate School of Pharmaceutical Sciences, Kyushu University, 3-1-1 Maidashi, Higashi-ku, Fukuoka 812-8582, Japan. Phone: 81-92-642-6296; Fax: 81-92-642-6296; E-mail: mono@phar.kyushu-u.ac.jp.

doi:10.1158/0008-5472.CAN-08-4882

Plasmid constructs. To obtain full-length cDNA of human IKKβ, PCR was carried out on a SuperScript cDNA library (Invitrogen) using the following primer pairs: 5′-ATGAGCTGGTCACCTTCCCTGACAAC-3′ and 5′-TCATGAGGCCTGCTCCAGGCAGCTG-3′ (IKKβ). The PCR product was ligated into the pGEM-T easy vector (Promega), and Flag-IKKβ was ligated into the p3xFLAG-CMV10 vector (Sigma).

Oligonucleotide microarray analysis. Duplicate samples were prepared for microarray hybridization. Total RNA (2 μg) was reverse transcribed using a GeneChip 3′-Amplification Regents One Cycle cDNA Synthesis kit (Affymetrix) and labeled with Cy5 or Cy3. The labeled cRNA was applied to the oligonucleotide microarray (Human Genome U133 Plus 2.0 Array; Affymetrix), the microarray was scanned on a GeneChip Scanner3000, and the image was analyzed using GeneChip Operating Software version 1 as described previously (15).

Determination of melanoma growth-stimulating activity α/CXCL1, epithelial-derived neutrophil activating protein-78/CXCL5, IL-8/CXCL8, and VEGF-A levels by ELISA. The concentrations of IL-8/CXCL8, VEGF-A, melanoma growth-stimulating activity α (Groα)/CXCL1, and epithelial-derived neutrophil activating protein-78 (ENA-78)/CXCL5 in the homogenized supernatant of mouse xenograft tumors and conditioned medium were measured using commercially available ELISA kits (R&D Systems) in accordance with the manufacturer's instructions.

EMSA. EMSA was done as follows. Nuclear extract (6 μg) was incubated for 15 min at room temperature with a 1×10^4 counts/min ^{32}P-labeled oligonucleotide probe in binding buffer [10 mmol/L HEPES-NaOH (pH 7.9), 1 mmol/L EDTA, 50 mmol/L NaCl, 10% glycerol, 0.1 mg/mL bovine serum albumin, 0.05% NP-40, 0.005 mg/mL DTT, 0.05 mg/mL poly(deoxyinosinic-deoxycytidylic acid)] as described previously (16). The reaction mixtures were separated on a nondenaturing 4% polyacrylamide gel, and radioactivity was detected with a FLA 5000 image analyzer (Fuji Film).

Immunoprecipitations and Western blotting. The cells treated with or without MG-132 (10 μmol/L) under 2% serum condition for 8 h were lysed in lysis buffer [50 mmol/L Tris-HCl (pH 8.0), 250 mmol/L NaCl, 0.3% NP-40, 1 mmol/L EDTA, 10% glycerol, 0.1 mmol/L Na_3VO_4] supplemented with a mixture of protease inhibitors. Lysates were incubated with anti-ubiquitin antibody for 2 h at 4°C and with protein A/G agarose for additional 1 h. After all immunoprecipitates were washed three times with lysis buffer, Western blotting was done with anti-IKKβ antibody as described previously (17). The intensity of the luminescence was quantified using a CCD camera combined with an image analysis system (LAS-1000; Fuji Film).

Animals. All animal experiments were approved by the Ethics of Animal Experiments Committee at Kyushu University Graduate School of Medical Sciences. Male athymic *nu/nu* mice were purchased from Charles River Laboratories and housed in microisolator cages maintained under a 12-h light/dark cycle. Water and food were supplied *ad libitum*. Animals were observed for signs of tumor growth, activity, feeding, and pain in accordance with the guidelines of the Harvard Medical Area Standing Committee on Animals.

Immunohistochemical analysis. MIApaca-2 transfectants were injected subcutaneously into mice (1.0×10^7 cells/0.1 mL/mouse). At day 49 after transplantation of MIApaca-2 transfectants, the tumors were fixed and immunohistochemical analysis was done as described previously (5, 18). All human tissue samples were fixed and embedded in paraffin, and immunohistochemical analysis was done as described previously (5, 18). In all tissue samples, the mean value of the number of infiltrating macrophages and neutrophils and the MVD were calculated from four or five hotspots. All counts were done by three independent observers.

Statistical analysis. Data are expressed as mean ± SD. All calculations (Welch's *t* test, Student's *t* test, and Wilcoxon/Kruskal-Wallis test) were done using JMP version 5.0 (SAS Institute).

Patients and specimens. Surgically respected specimens from 37 patients with pancreatic ductal adenocarcinoma were studied. All patients underwent surgical resection between 1991 and 1998 at the Department of Surgery, Kurume University Hospital. Informed consent was obtained from all patients, and the study protocol was approved by the Ethics Committee of Kurume University.

Results

NDRG1/Cap43 down-regulates the expression of angiogenesis- and inflammation-related genes. To understand how NDRG1/Cap43 modulates tumor angiogenesis and growth in pancreatic cancer cells, we compared the expression profiles of NDRG1/Cap43 transfectant (Cap#11) and the parental low-expression counterpart (Mock#2) of MIApaca-2 cells using a high-density oligonucleotide microarray (Supplementary Table S1).

We selected eight genes predicted to be associated with adhesion, growth, and chemotaxis (Supplementary Table S2). Because our previous study showed that NDRG1/Cap43 overexpression in pancreatic cancer cells reduced the expression of angiogenesis-related factors such as VEGF-A and IL-8/CXCL8 (5), we also selected these genes, the expression of which showed a decrease of ~0.7 (Supplementary Table S2).

We confirmed the expression of NDRG1/Cap43 in two NDRG1/Cap43 transfectants (Cap#11 and Cap#14) and their mock transfectants (Mock#2) of MIApaca-2 cells (Fig. 1*A*). We compared the expression of these genes in high- and low-NDRG1/Cap43-expressing MIApaca-2 cells by quantitative real-time PCR. From the array results, we selected NCAM1, which was up-regulated by NDRG1/Cap43, as a control. The mRNA expression levels of Groα/CXCL1, ENA-78/CXCL5, IL-8/CXCL8, and VEGF-A were significantly decreased in two NDRG1/Cap43 transfectants (Cap#11 and Cap#14) in comparison with Mock#2 cells (Supplementary Fig. S1).

We used ELISA assays to compare protein levels of chemokines among pancreatic cancer cells showing low and high expression of NDRG1/Cap43 (Fig. 1*B*). We observed that Cap#11 and Cap#14 cells showed a marked decrease in the production of Groα/CXCL1 and ENA-78/CXCL5 as well as IL-8/CXCL8.

NDRG1/Cap43 suppresses the NF-κB signaling pathway in pancreatic cancer cells. Representative angiogenic factors such as IL-8/CXCL8 and VEGF-A are regulated by NF-κB (19). We investigated whether NDRG1/Cap43 expression interfered with the NF-κB signaling pathway in pancreatic cancer cells. The phosphorylation of IκBα was activated in Mock#2 cells cultured in the presence of 2% serum compared with Cap#11 and Cap#14 cells (Fig. 1*C*, *left*). By contrast, in the absence of serum, there appeared to be weak activation of IκBα in Mock#2 cells. However, NDRG1/Cap43 expression level was not affected with or without serum in NDRG1/Cap43 transfectants (Fig. 1*C*, *left*). Next, we determined the expression levels of proteins related to the NF-κB signaling pathway to examine which molecules are responsible for the difference in the phosphorylation level of IκBα between NDRG1/Cap43 and mock transfectants. Phosphorylation of IκBα is regulated by the IKK complex, which consists of two catalytic subunits, IKKα and IKKβ, and a regulatory component, IKKγ/NEMO. The expression of IKKβ was markedly reduced in Cap#11 and Cap#14 cells compared with Mock#2 cells (Fig. 1*C*, *middle*). There were no differences in the expression levels of other NF-κB signaling pathway-related proteins (NIK, TAB1/2, TAK1, IKKα, and IKKγ) between NDRG1/Cap43 and mock transfectants, and the expression levels of NF-κB subunits such as p65, p50, RelB, and p52 in Cap#11 and Cap#14 cells were similar to those in Mock#2 cells (Fig. 1*C*, *right*). Expression of IKKβ mRNA is slightly, but not significantly, decreased in NDRG1/Cap43 transfectants (Supplementary Fig. S2). In Cap#11 and Cap#14 cells, nuclear translocation of p65 was decreased by ~50% to 70% and that of p50 was decreased by ~80% compared with Mock#2, respectively (Fig. 1*D*, *left*). Expression of p65 and p50 showed only a slight increase in

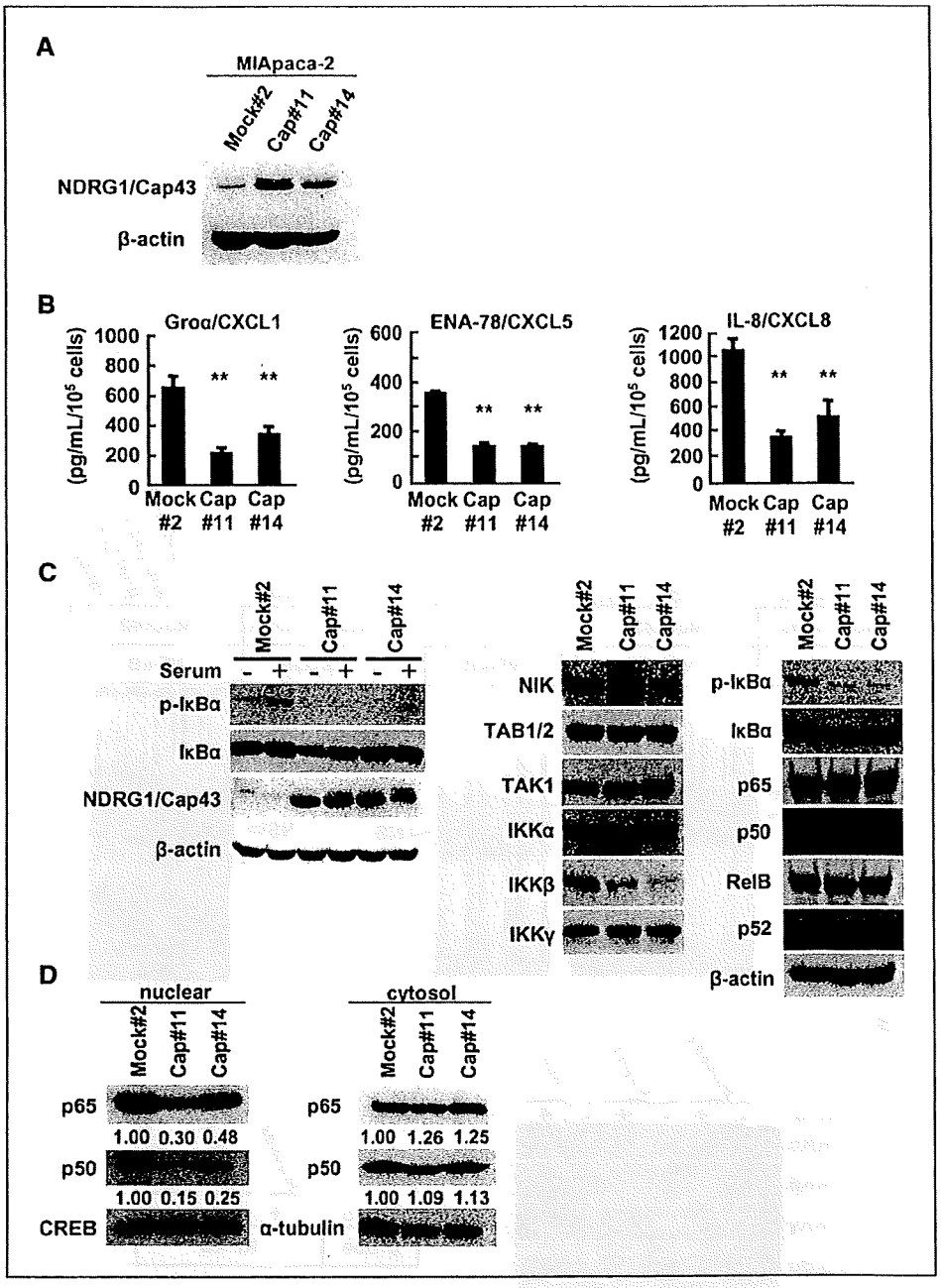

Figure 1. NDRG1/Cap43 reduces expression levels of CXC chemokines and phosphorylation of IκBα in MIApaca-2 cell lines showing low and high NDRG1/Cap43 expression. All experiments, except *A*, were done with 2% serum for 24 h. *A*, Western blot analysis of NDRG1/Cap43 expression in MIApaca-2 transfectants. *B*, ELISA assay analysis of Groα/CXCL1, ENA-78/CXCL5, and IL-8/CXCL8 protein levels in NDRG1/Cap43 and mock transfectants of MIApaca-2 cells. *Columns*, mean of three independent experiments; *bars*, SE. **, $P < 0.01$ versus Mock#2 cells. *C*, phosphorylation of IκBα and NDRG1/Cap43 expression in NDRG1/Cap43 and mock transfectants cultured with or without 2% serum for 24 h was measured by Western blotting (*left*). Western blot analysis of the expression of NF-κB signaling pathway-related proteins using whole-cell lysates prepared from NDRG1/Cap43 and mock transfectants (*middle* and *right*). *D*, Western blot analysis of the expression of p65 and p50 in nuclear (*left*) and cytosol (*right*) extracts prepared from NDRG1/Cap43 and mock transfectants. Levels of protein expression are expressed relative to the level of p65 or p50 protein in Mock#2, which is presented as 1.00.

cytosol fraction of Cap#11 and Cap#14 compared with that of Mock#2 (Fig. 1*D*, *right*).

We next performed EMSA to assess whether NDRG1/Cap43 altered the binding ability of NF-κB. One major shifted protein-DNA complex was observed after incubation of nuclear extracts prepared from Mock#2 cultured with 2% serum for 24 h (Fig. 2*A*). These complexes were specifically competed out with a 2-fold excess of the same unlabeled oligonucleotide but not with an unlabeled TRE and GC-box oligonucleotide. The protein-DNA complex after incubation of nuclear extracts was markedly decreased in Cap#11 and Cap#14 compared with Mock#2 when cultured with 2% serum. When protein-DNA complexes were incubated with antibodies against p65 and p50, supershifted bands were observed in Mock#2 (Fig. 2*A*). We next examined whether the reduced level of p-IκBα could be restored by a potent inflammatory cytokine, TNF-α, in NDRG1/Cap43 transfectants (Fig. 2*B*). TNF-α induced phosphorylation of IκBα in both Cap#11 and Cap#14 at similar levels as their parental counterpart. However, cellular levels of IKKβ in Cap#11 and Cap#14 were not affected by TNF-α. Figure 2*C* shows that TNF-α also restored the expression of IL-8/CXCL8 in Cap#11 and Cap#14 cells to levels comparable with those in Mock#2 cells. Treatment with TNF-α also enhanced the affinity of p65 and p50 for NF-κB binding sites in Cap#11 and Cap#14 at similar levels to those in their parental counterparts (Fig. 2*D*). Taken together, NDRG1/Cap43 was not involved in TNF-α-induced NF-κB signaling pathway.

IKKβ overexpression overcomes NDRG1/Cap43-induced suppression of IκBα phosphorylation and chemokine expression. Expression of IKKβ was decreased in two NDRG1/Cap43 transfectants (Cap#11 and Cap#14). We examined whether exogenous IKKβ expression was able to restore the IκBα phosphorylation in NDRG1/Cap43 transfectants. Expression of IKKβ was augmented in both NDRG1/Cap43 and mock transfectants after transfection of the exogenous IKKβ gene (Fig. 3*A*). The phosphorylation of IκBα was increased in Cap#11 to a level comparable with that in Mock#2. Expression of Groα/CXCL1, ENA-78/CXCL5, and IL-8/CXCL8 was also significantly increased after transfection of IKKβ in Cap#11 cells when there was no apparent difference in the expression levels of these chemokines between empty and IKKβ transfection in Mock#2 (Fig. 3*B*). Expression of VEGF-A was also increased in IKKβ-transfected Cap#11 cells compared with that in empty-transfected Cap#11 cells. We observed that VEFG-A expression was decreased in IKKβ-transfected Mock#2 compared with empty-transfected Mock#2 cells, but the reason for this remains unclear.

IKKβ has been reported to hold a putative ubiquitin-like domain (20). We examined whether the reduced expression of IKKβ protein was restored by proteasome inhibitor, MG-132, in Cap#11 cells. MG-132 inhibited degradation of p-IκBα in both Mock#2 and Cap#11 cells (Fig. 3*C*). Furthermore, expression of IKKβ in Cap#11 cells was restored to similar levels as in Mock#2 cells when treated with MG-132. MG-132 did not significantly affect IKKβ mRNA expression in Mock#2 ($P = 0.65$) and Cap#11 ($P = 0.48$) cells

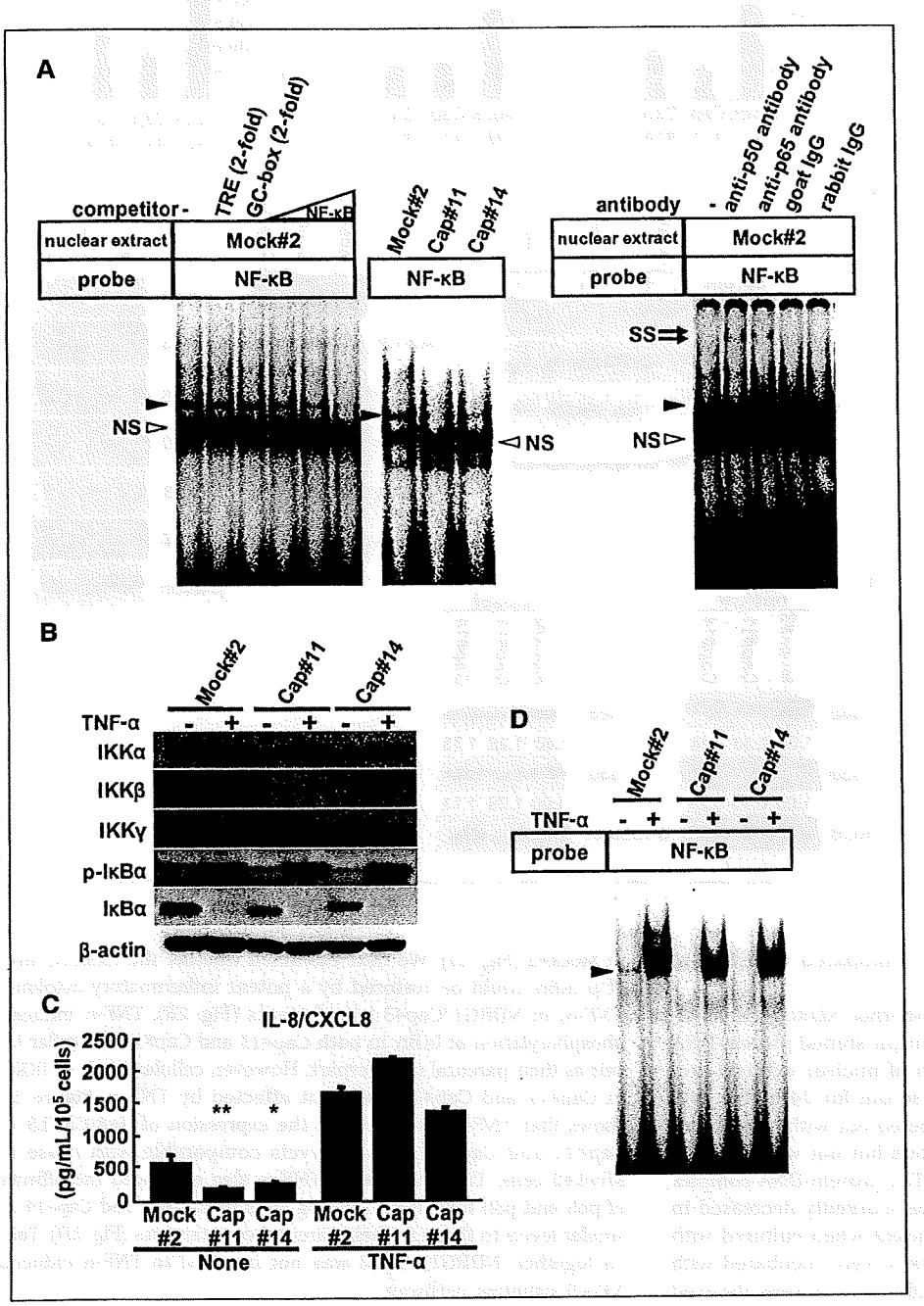

Figure 2. Suppression of binding activity of NF-κB by NDRG1/Cap43. *A*, EMSA using the NF-κB binding oligonucleotide. Nuclear extracts from three transfectants cultured in the presence of 2% serum were incubated with oligonucleotide as described in Materials and Methods. *Black arrowheads*, shifted bands; 0.08-, 0.4-, or 2-fold molar excess of unlabeled oligonucleotide was used as the competitor. A 2-fold molar excess of unlabeled oligonucleotide (TRE and GC-box) was used as a negative control for this competition assay. *Arrows*, positions of the supershifted bands (*SS*); *NS*, nonspecific band (*white arrowheads*). *B*, Western blot analysis of IκBα phosphorylation and expression of IKKα, IKKβ, and IKKγ in NDRG1/Cap43 and mock transfectants under serum-free conditions with or without TNF-α (20 ng/mL) stimulation for 30 min. *C*, ELISA assay analysis of IL-8/CXCL8 protein levels in NDRG1/Cap43 and mock transfectants of MIApaca-2 cells under serum-free conditions with or without TNF-α (20 ng/mL) for 24 h. *Columns*, mean of three independent experiments; *bars*, SE. *, $P < 0.05$; **, $P < 0.01$ versus mock transfectants. *D*, EMSA using the NF-κB binding oligonucleotide with nuclear extracts from three transfectants under serum-free conditions with or without TNF-α (20 ng/mL) for 30 min. *Black arrowheads*, shifted bands.

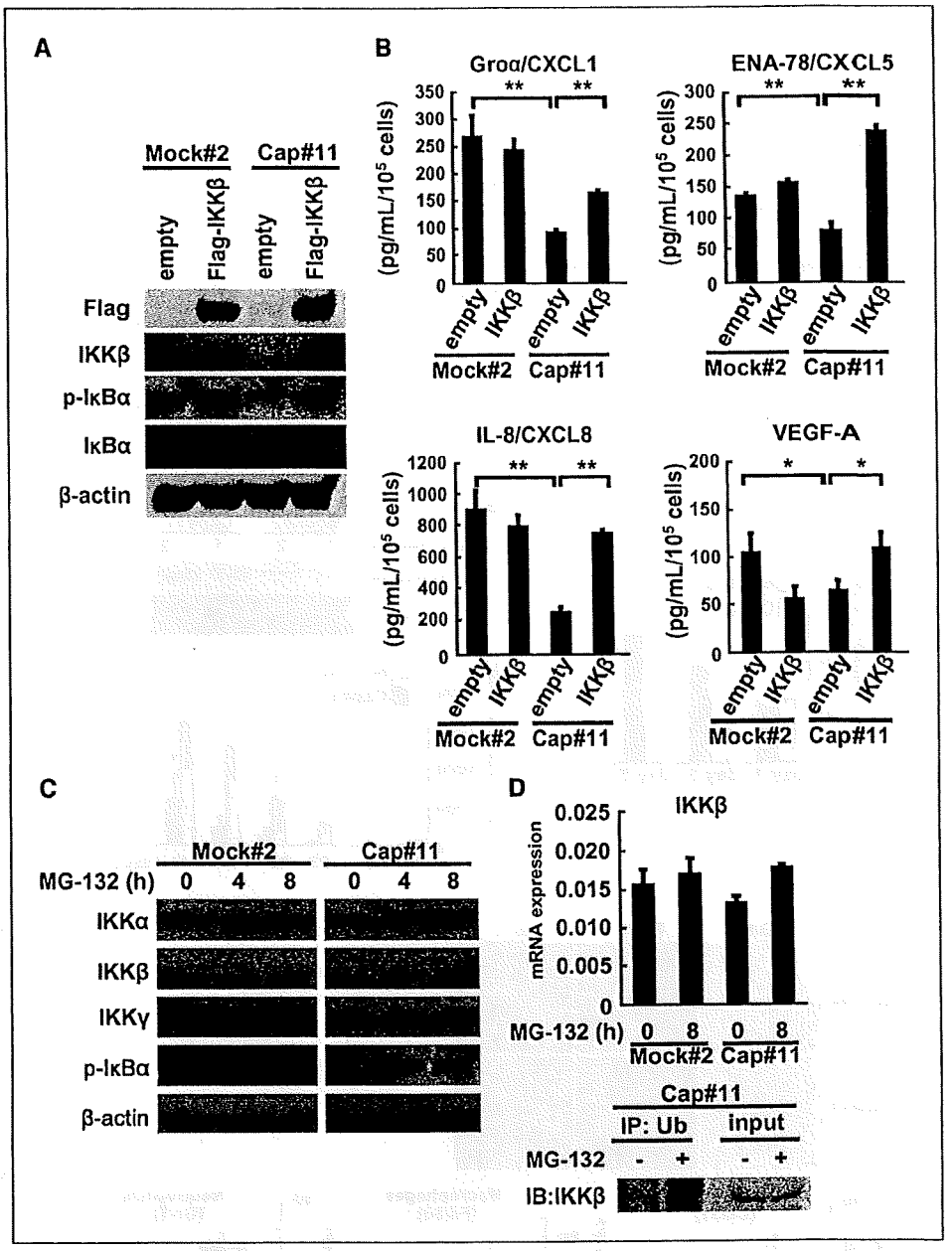

Figure 3. IKKβ overexpression restores the level of p-IκBα and expression of the CXC chemokines and VEGF-A. *A*, expression of the exogenous IKKβ gene and phosphorylation of IκBα in MIApaca-2 transfectants. NDRG1/Cap43 and mock transfectants were transiently transfected with the IKKβ expression vector. At 30 h after IKKβ transfection, the cells were again seeded and cultured for 18 h and then cultured in medium containing 2% serum for 24 h. *B*, ELISA assay analysis of Groα/CXCL1, ENA-78/CXCL5, IL-8/CXCL8, and VEGF-A protein levels in Mock#2 and Cap#11 that were transfected with the IKKβ expression vector. At 48 h after IKKβ transfection, the cells were cultured in medium containing 2% serum for 24 h. *Columns*, mean of three independent experiments; *bars*, SE. *, $P < 0.05$; **, $P < 0.01$ versus empty-transfected Cap#11 cells. *C*, Western blot analysis of IκBα phosphorylation and IKKα, IKKβ, and IKKγ expression in NDRG1/Cap43 and mock transfectants treated with MG-132 (10 μmol/L) in the presence of 2% serum for indicated time. *D*, quantitative real-time PCR analysis of IKKβ mRNA levels in NDRG1/Cap43 and mock transfectants treated with MG-132 (10 μmol/L) in the presence of 2% serum for the indicated time. *Columns*, mean of three independent experiments; *bars*, SE (*top*). Cells were treated with or without MG-132 (10 μmol/L) for 8 h before lysis. Immunoprecipitation was done with anti-ubiquitin (*Ub*) antibody and immunoblotting was with anti-IKKβ antibody (*bottom*).

(Fig. 3*D*, *top*). We further examined whether IKKβ was ubiquitinated or not in the presence of MG-132. As shown in Fig. 3*D* (*bottom*), ubiquitination of IKKβ was shown in Cap#11 cells, suggesting that a proteasomal degradation plays a role in down-regulation of IKKβ in the NDRG/Cap43-expressing cells.

NDRG1/Cap43 suppresses infiltration of inflammatory cells, expression of angiogenesis-related factors, tumor growth, and tumor angiogenesis. Consistent with our previous study (5), there was no difference in growth rates among Mock#2 and Cap#11 cells in culture (Fig. 4*A*). By contrast, tumor growth of Cap#11 was markedly reduced in comparison with Mock#2 in a subcutaneous mouse xenograft model (Fig. 4*B*, *bottom*). Immunoblotting analysis showed that NDRG1/Cap43 protein was consistently and highly expressed in Cap#11 tumors on day 49 after inoculation compared with Mock#2 tumors (Fig. 4*B*, *top*).

NDRG1/Cap43 was found to reduce the expression of chemokines and growth factors that function in chemotaxis of monocytes/macrophages and neutrophils (Fig. 1*B*; Supplementary Fig. S1). Mock#2 and Cap#11 tumor sections were further analyzed by immunohistochemistry for expression of microvessels (CD31), macrophages (F4/80), and neutrophils (Gr-1; Fig. 4*C*, *top*). MVD staining showed a markedly higher number of tumor neovessels in Mock#2 tumors than in Cap#11 tumors on day 49 after implantation (Fig. 4*C*, *bottom*). There appeared to be much lower infiltration of F4/80-positive macrophages and also Gr-1-positive infiltrating neutrophils in the stroma of Cap#11 tumors compared with that of Mock#2 tumors (Fig. 4*C*, *bottom*). NDRG1/Cap43 expression was thus closely associated with decreased MVD and also with a decreased number of infiltrating macrophages and neutrophils in mouse xenograft tumors. Expression of IL-8/CXCL8 and

VEGF-A was significantly reduced in Cap#11 tumors compared with Mock#2 tumors (Fig. 4*D*), suggesting that reduced expression of such chemokines and growth factors was continuously maintained during tumor growth in this mouse xenograft model.

Association of NDRG1/Cap43 expression level with infiltrating inflammatory cells in tumors of pancreatic cancer patients. Expression of NDRG1/Cap43 was previously shown to be inversely correlated with MVD in the tumors of patients with pancreatic cancer (5). Based on the expression level of NDRG1/Cap43 in resected specimens from 37 patients with pancreatic ductal adenocarcinoma, we divided them into two groups: NDRG1/Cap43 positive (n = 18) and NDRG1/Cap43 negative (n = 19). Supplementary Table S3 shows the association between NDRG1/Cap43 expression and clinicopathologic variables such as age, gender, depth of invasion, lymph node metastasis, and pathologic stage in patients with pancreatic ductal adenocarcinoma. High NDRG1/Cap43 expression was significantly correlated with invasion depth (Supplementary Table S3).

In the human tumor stroma, some cases showed a lower number of infiltrating CD68$^+$ macrophages/monocytes in NDRG1/Cap43-positive pancreatic cancer (Fig. 5*A*, *a* and *b*), whereas others showed a higher number of infiltrating CD68$^+$ macrophages/monocytes in NDRG1/Cap43-negative pancreatic cancer (Fig. 5*A*, *c* and *d*). Quantitative analysis indicated that the number of infiltrating macrophages/monocytes was relatively higher in patients with NDRG1/Cap43-negative tumors than in those with NDRG1/Cap43-positive tumors (Fig. 5*A*, *right*), the mean number of infiltrating macrophages/monocytes being 97.5 and 62.3, respectively. However, similar numbers of infiltrating neutrophils were observed in the tumor stroma of patients with NDRG1/Cap43-positive and

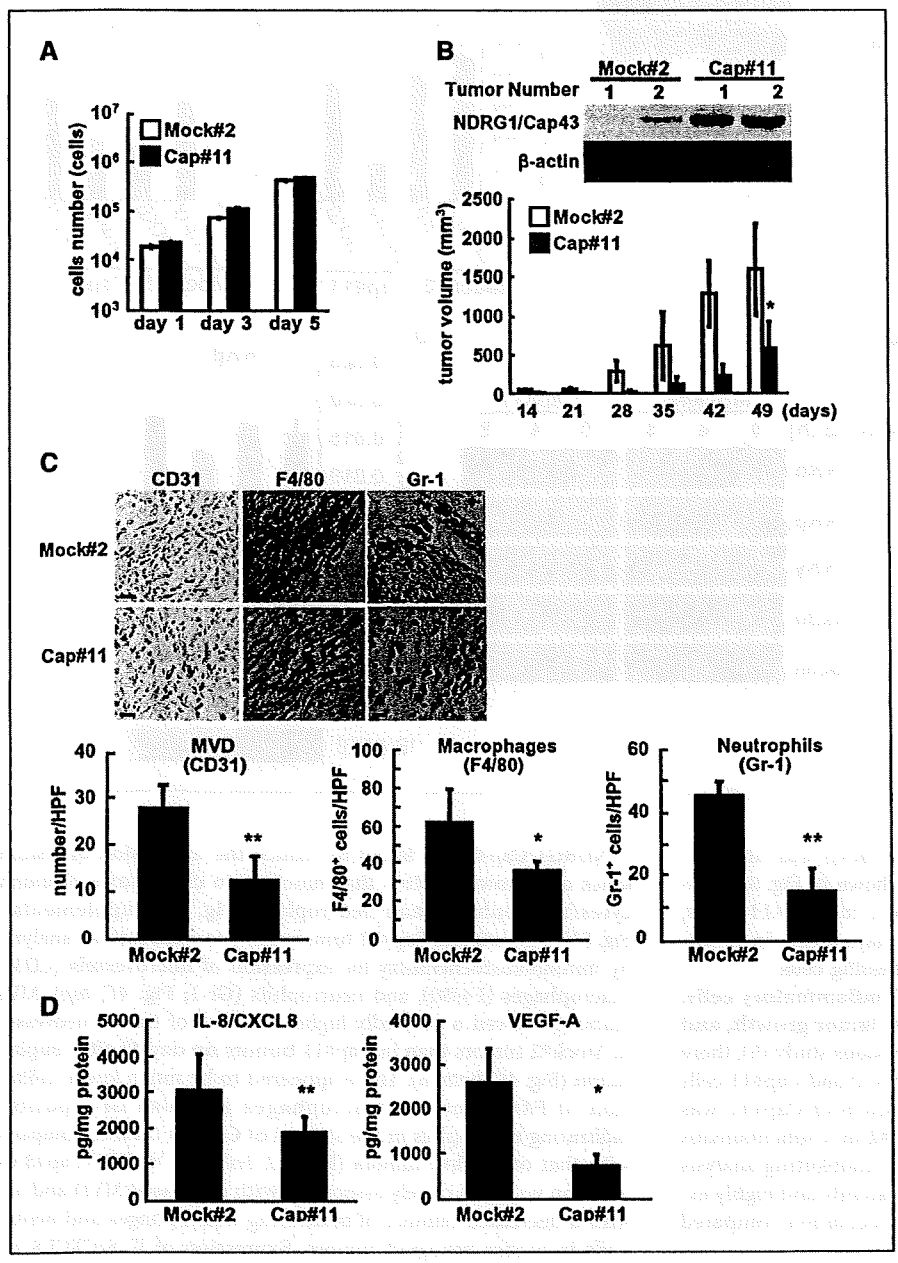

Figure 4. NDRG1/Cap43 represses MVD and the number of infiltrating macrophages or neutrophils in mouse subcutaneous tumors. *A*, comparison of cell proliferation in MIApaca-2 transfectant cells (Mock#2 and Cap#11). Cells were seeded on day 0 at 1.0×10^4 per well and cultured in DMEM with 10% serum. Cell growth was measured on days 1, 3, and 5. *Columns*, mean of three independent experiments; *bars*, SE. *B*, Western blot analysis of NDRG1/Cap43 expression in tumors comprising Mock#2 or Cap#11 cells on day 49 (*top*). *Columns*, mean tumor volumes; *bars*, SE. Tumor volumes were determined every week after tumor implantation (n = 5 or 6; *bottom*). *C*, immunohistochemical analysis. Representative photographs of tumor sections stained with the anti-CD31, anti-F4/80, and anti-Gr-1 antibodies from Mock#2 and Cap#11 xenografts on day 49. *Bar*, 25 μm (*top*). Mean MVD for tumor sections from Mock#2 and Cap#11 xenografts on day 49 was determined by counting the number of CD31$^+$ vessels in the tumors. Mean numbers of infiltrating macrophages and neutrophils in tumor sections from Mock#2 and Cap#11 xenografts on day 49 were determined by counting the intensity of F4/80- or Gr-1-positive cells in the tumor stroma. *Columns*, mean; *bars*, SE (n = 5; *bottom*). *HPF*, high-power field. *D*, ELISA assay analysis of human IL-8/CXCL8 and VEGF-A protein levels in Mock#2 and Cap#11 tumors. *Columns*, mean; *bars*, SE (n = 4). *, $P < 0.05$; **, $P < 0.01$ versus Mock#2 tumors.

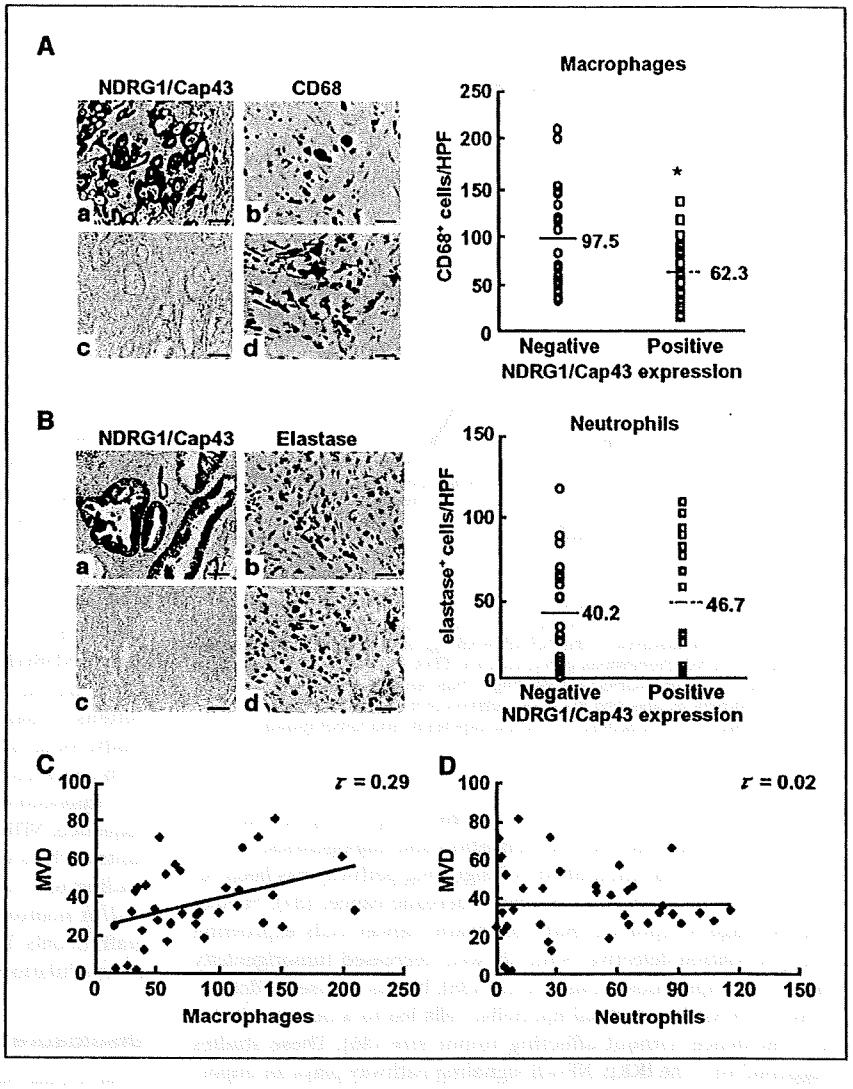

Figure 5. NDRG1/Cap43 expression levels and numbers of infiltrating inflammatory cells in human pancreatic cancer. *A*, immunohistochemical analysis of macrophages in tumor stroma using the anti-NDRG1/Cap43 antibody and anti-CD68 antibody. Representative photographs showing low infiltration of macrophages in NDRG1/Cap43-positive specimens (*a* and *b*). Representative photographs showing high infiltration of macrophages in NDRG1/Cap43-negative specimens (*c* and *d*). *Bar*, 50 μm (*a* and *c*) and 25 μm (*b* and *d*). Correlation between NDRG1/Cap43 expression levels and numbers of infiltrating macrophages. Mean number of infiltrating macrophages was 97.5 in NDRG1/Cap43-negative specimens ($n = 19$) and 62.3 in NDRG1/Cap43-positive specimens ($n = 18$; *right*). *, $P < 0.05$. *B*, immunohistochemical analysis of neutrophils in tumor stroma using an anti-NDRG1/Cap43 antibody and anti-elastase antibody. Representative photographs of neutrophils infiltration in NDRG1/Cap43-positive specimens (*a* and *b*) and NDRG1/Cap43-negative specimens (*c* and *d*). Correlation between NDRG1/Cap43 expression level and number of infiltrating neutrophils. Mean number of infiltrating neutrophils was 40.2 in NDRG1/Cap43-negative specimens and 46.7 in NDRG1/Cap43-positive specimens (*right*). *C* and *D*, correlation between MVD and number of infiltrating macrophages or neutrophils in patients with pancreatic ductal adenocarcinoma ($n = 37$). $r = 0.29$ and 0.02, Kendall correlation coefficient.

NDRG1/Cap43-negative pancreatic cancer (Fig. 5*B*). Quantitative analysis showed that the mean number of infiltrating neutrophils was 40.2 in NDRG1/Cap43-negative specimens and 46.7 in NDRG1/Cap43-positive specimens, with no significant difference (Fig. 5*B*, *right*).

Our previous study showed that NDRG1/Cap43 expression levels were inversely correlated with MVD (5). Therefore, we further examined whether infiltration of macrophages/monocytes and neutrophils was associated with MVD in patients with NDRG1/Cap43-positive and NDRG1/Cap43-negative pancreatic cancer ($n = 37$). The number of infiltrating macrophages/monocytes was positively correlated with MVD (Fig. 5*C*; $P < 0.05$). However, there was no correlation between the number of infiltrating neutrophils and the MVD (Fig. 5*D*).

Discussion

We reported previously that NDRG1/Cap43 overexpression suppressed the expression of VEGF-A, IL-8/CXCL8, and matrix metalloproteinase-9 in pancreatic cancer cells (5). In the present study, we showed that NDRG1/Cap43 down-regulated the expression of several other genes, including chemoattractants for inflammatory cells. We also observed that decreased expression of IL-8/CXCL8 and VEGF-A in mouse tumors was associated with high expression of NDRG1/Cap43. These chemoattractants down-regulated by NDRG1/Cap43 had chemotactic effects on monocytes/macrophages and neutrophils. Our results showed that overexpression of NDRG1/Cap43 resulted in marked decrease in infiltration of macrophages and neutrophils in xenograft models.

One critical step in progression from a benign to a malignant state is angiogenesis. Infiltration of activated fibroblasts (21), macrophages/monocytes (22), and neutrophils (23) is expected to play a key role in the angiogenic switch of cancer (23–25). From our laboratory, we have also reported that infiltration of macrophages in the tumor stroma markedly promoted angiogenesis through the secretion of various proangiogenic cytokines and extracellular matrix-degrading proteases (18, 26–29). Groα/CXCL1, ENA-78/CXCL5, and IL-8/CXCL8 play an important role in tumor-associated angiogenesis and tumorigenesis in cancers of the kidney, pancreas, head and neck, and lung (30–33). Also, expression of CXC chemokines and VEGF-A would thus be expected to be closely involved in NDRG1/Cap43-induced suppression of tumor angiogenesis (Fig. 6). However, it is important to elucidate in more detail the underlying mechanism by which cytokines and growth

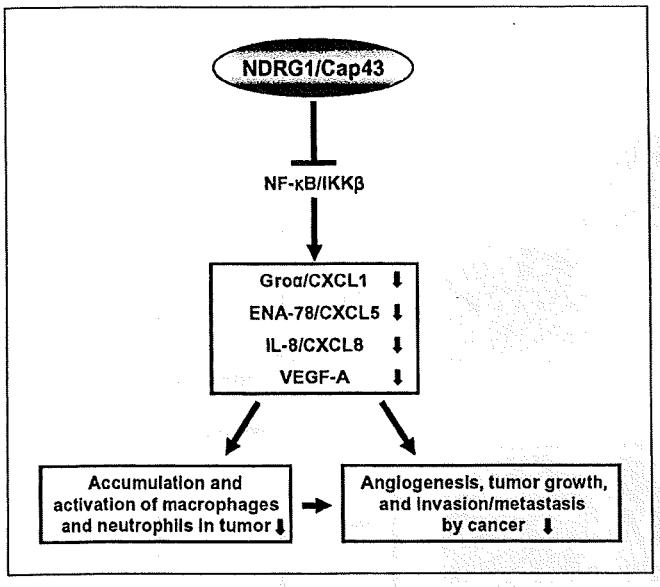

Figure 6. NDRG1/Cap43 plays a critical role as an antiangiogenic regulator through modulation of the tumor microenvironment in pancreatic cancer. NDRG1/Cap43 attenuates activation of the NF-κB/IKKβ signaling, resulting in decreased expression of CXC chemokines (Groα/CXCL1, ENA-78/CXCL5, and IL-8/CXCL8) and VEGF-A. NDRG1/Cap43 might thus remodel the tumor microenvironment by affecting the accumulation of inflammatory cells (macrophages and neutrophils), tumor angiogenesis, and tumor growth.

factors are directly involved in the NDRG1/Cap43-dependent suppression of inflammatory cell infiltration and angiogenesis.

Constitutive activation of NF-κB signaling pathway has been reported in many cancers, including pancreatic cancer (34). Fujioka and colleagues reported that pancreatic cancer cells expressing phosphorylation-defective IκBα showed decreased tumorigenicity in an orthotopic nude mouse model (35). In this mouse model, deletion of IKKβ in intestinal epithelial cells led to a decrease in tumor incidence without affecting tumor size (36). These studies suggested that the IKKβ-NF-κB signaling pathway plays an important role in tumor development.

In our present study, NDRG1/Cap43 reduced the expression of p-IκBα and its upstream regulator IKKβ in pancreatic cancer cells. However, we found no apparent phosphorylation of IKKα and IKKβ in NDRG1/Cap43 and mock transfectants under 2% serum condition (data not shown), suggesting that decreased expression of IKKβ is responsible for the loss of p-IκBα in NDRG1/Cap43 transfectants. The loss of p-IκBα results in reduction of both nuclear translocation of p65 and p50 and their binding to the NF-κB motif. NDRG1/Cap43-induced suppression of IKKβ was almost completely restored by a proteasome inhibitor. Introduction of an exogenous IKKβ gene was able to restore IκBα phosphorylation and expression of Groα/CXCL1, ENA-78/CXCL5, IL-8/CXCL8, and VEGF-A in NDRG1/Cap43 transfectants. In this study, we also found ubiquitination of IKKβ in NDRG1/Cap43 transfectant. A relevant study by May and colleagues showed that a ubiquitin-like domain of IKKβ is required for its functional activation (20). Taken together, the IKKβ-NF-κB pathway is expected to be attenuated by NDRG1/Cap43, resulting in decreased expression of angiogenesis and chemotaxis-related factors (see Fig. 6).

In various solid human tumors, an increase in the number of infiltrating tumor-associated macrophages has been shown to be closely associated with not only prognosis but also tumor angiogenesis (29, 37, 38). In our present study, a significantly decreased number of macrophages was also observed in clinical specimens of pancreatic cancer showing relatively higher NDRG1/Cap43 expression. The number of infiltrating macrophages was correlated with neovascularization in patients with pancreatic cancer. By contrast, we did not observe any significant difference in the number of infiltrating neutrophils between human pancreatic cancers showing low and high expression of NDRG1/Cap43. As shown in Fig. 4, in mouse xenograft models, chemotaxis of neutrophils and macrophages/monocytes was suppressed in Cap#11 xenograft. By contrast, in clinical specimens of pancreatic cancer, infiltration of macrophages, but not neutrophils, was significantly associated with higher NDRG1/Cap43 expression. It remains unclear why NDRG1/Cap43 has no effect on the infiltration of neutrophils in clinical specimens of pancreatic cancer, and this question requires further study, focusing particularly on pancreatic cancer at earlier stages.

In conclusion, this study has shown that NDRG1/Cap43 decreases the expression of IKKβ and the NF-κB signaling pathway. As a consequence, NDRG1/Cap43 decreases the expression of chemoattractants such as CXC chemokines and VEGF-A for inflammatory cells, leading to a marked decrease in the recruitment of macrophages and/or neutrophils, along with angiogenesis suppression, in xenograft models. Therefore, NDRG1/Cap43 could be a potent biomarker for modulation of the tumor stroma in pancreatic cancer.

Disclosure of Potential Conflicts of Interest

No potential conflicts of interest were disclosed.

Acknowledgments

Received 12/22/08; revised 3/12/09; accepted 4/17/09; published OnlineFirst 6/2/09.

Grant support: Grants-in-aid for Scientific Research in Priority Areas of Cancer from the Ministry of Education Culture, Sports Science, and Technology of Japan (M. Ono), Third-Term Comprehensive Control Research for Cancer from the Ministry of Health, Labor and Welfare, Japan (M. Kuwano), and Formation of Innovation Center for Fusion of Advanced Technologies, Kyushu University (M. Ono and M. Kuwano), and JSPS-Asia Core Program (M. Ono).

The costs of publication of this article were defrayed in part by the payment of page charges. This article must therefore be hereby marked *advertisement* in accordance with 18 U.S.C. Section 1734 solely to indicate this fact.

We thank Drs. K. Matsuo, T. Utsugi (Hanno Research Center for Taiho Parmaceutical), Y. Maruyama, and Y. Basaki (Kyushu University) for fruitful discussions.

References

1. Berger JC, Vander Griend DJ, Robinson VL, Hickson JA, Rinker-Schaeffer CW. Metastasis suppressor genes: from gene identification to protein function and regulation. Cancer Biol Ther 2005;4:805–12.
2. Kovacevic Z, Richardson DR. The metastasis suppressor, Ndrg-1: a new ally in the fight against cancer. Carcinogenesis 2006;27:2355–66.
3. Guan RJ, Ford HL, Fu Y, Li Y, Shaw LM, Pardee AB. Drg-1 as a differentiation-related, putative metastatic suppressor gene in human colon cancer. Cancer Res 2002;60:749–55.
4. Bandyopadhyay S, Pai SK, Gross SC, et al. The Drg-1 gene suppresses tumor metastasis in prostate cancer. Cancer Res 2003;63:1731–6.
5. Maruyama Y, Ono M, Kawahara A, et al. Tumor growth suppression in pancreatic cancer by a putative metastasis suppressor gene Cap43/NDRG1/Drg-1 through modulation of angiogenesis. Cancer Res 2006; 66:6233–42.
6. Fotovati A, Fujii T, Yamaguchi M, et al. 17β-Estradiol induces down-regulation of Cap43/NDRG1/Drg-1, a putative differentiation-related and metastasis suppressor gene, in human breast cancer cells. Clin Cancer Res 2006;12:3010–8.
7. Bandyopadhyay S, Pai SK, Hirota S, et al. Role of the

putative tumor metastasis suppressor gene Drg-1 in breast cancer progression. Oncogene 2004;23:5675–81.
8. Ando T, Ishiguro H, Kimura M, et al. Decreased expression of NDRG1 is correlated with tumor progression and poor prognosis in patients with esophageal squamous cell carcinoma. Dis Esophagus 2006;19:454–8.
9. Koshiji M, Kumamoto K, Morimura K, et al. Correlation of N-myc downstream-regulated gene 1 expression with clinical outcomes of colorectal cancer patients of different race/ethnicity. World J Gastroenterol 2007;213:2803–10.
10. Fukahori S, Yano H, Tsuneoka M, et al. Immunohistochemical expressions of Cap43 and Mina53 proteins in neuroblastoma. J Pediatr Surg 2007;42:1831–40.
11. Chua MS, Sun H, Cheung ST, et al. Overexpression of NDRG1 is an indicator of poor prognosis in hepatocellular carcinoma. Mod Pathol 2007;20:76–83.
12. Nishio S, Ushijima K, Tsuda N, et al. Cap43/NDRG1/Drg-1 is a molecular target for angiogenesis and a prognostic indicator in cervical adenocarcinoma. Cancer Lett 2008;264:36–43.
13. Nishie A, Masuda K, Otsubo M, et al. High expression of the Cap43 gene in infiltrating macrophages of human renal cell carcinomas. Clin Cancer Res 2001;7:2145–51.
14. Masuda K, Ono M, Okamoto M, et al. Downregulation of Cap43 gene by von Hippel-Lindau tumor suppressor protein in human renal cancer cells. Int J Cancer 2003;105:803–10.
15. Basaki Y, Hosoi F, Oda Y, et al. Akt-dependent nuclear localization of Y-box-binding protein 1 in acquisition of malignant characteristics by human ovarian cancer cells. Oncogene 2006;26:2736–46.
16. Izumi H, Ise T, Murakami T, et al. Structural and functional characterization of two human V-ATPase subunit gene promoters. Biochim Biophys Acta 2003;1628:97–104.
17. Ono M, Hirata A, Kometani T, et al. Sensitivity to gefitinib (Iressa, ZD1839) in non-small cell lung cancer cell lines correlates with dependence on the epidermal growth factor (EGF) receptor/extracellular signal-regulated kinase 1/2 and EGF receptor/Akt pathway for proliferation. Mol Cancer Ther 2004;3:465–72.
18. Nakao S, Kuwano T, Tsutsumi-Miyahara C, et al. Infiltration of COX-2-expressing macrophages is a prerequisite for IL-1β-induced neovascularization and tumor growth. J Clin Invest 2005;115:2979–91.
19. Maeda S, Omata M. Inflammation and cancer: role of nuclear factor-κB activation. Cancer Sci 2008;99:836–42.
20. May MJ, Larsen SE, Shim JH, Madge LA, Ghosh S. A novel ubiquitin-like domain in IκB kinase β is required for functional activity of the kinase. J Biol Chem 2004;279:45528–39.
21. Orimo A, Gupta PB, Sgroi DC, et al. Stromal fibroblasts present in invasive human breast carcinomas promote tumor growth and angiogenesis through elevated SDF-1/CXCL12 secretion. Cell 2005;121:335–48.
22. Condeelis J, Pollard JW. Macrophages: obligate partners for tumor cell migration, invasion, and metastasis. Cell 2006;124:263–6.
23. Nozawa H, Chiu C, Hanahan D. Infiltrating neutrophils mediate the initial angiogenic switch in a mouse model of multistage carcinogenesis. Proc Natl Acad Sci U S A 2006;103:12493–8.
24. Mahadevan D, Von Hoff DD. Tumor-stroma interactions in pancreatic ductal adenocarcinoma. Mol Cancer Ther 2007;6:1186–97.
25. Ardi VC, Kupriyanova TA, Deryugina EI, Quigley JP. Human neutrophils uniquely release TIMP-free MMP-9 to provide a potent catalytic stimulator of angiogenesis. Proc Natl Acad Sci U S A 2007;104:20262–7.
26. Torisu H, Ono M, Kiryu H, et al. Macrophage infiltration correlates with tumor stage and angiogenesis in human malignant melanoma: possible involvement of TNFα and IL-1α. Int J Cancer 2000;85:182–8.
27. Kuwano T, Nakao S, Yamamoto H, et al. Cyclooxygenase 2 is a key enzyme for inflammatory cytokine-induced angiogenesis. FASEB J 2004;18:300–10.
28. Kimura YN, Watari K, Fotovati A, et al. Inflammatory stimuli from macrophages and cancer cells synergistically promote tumor growth and angiogenesis. Cancer Sci 2007;98:2009–18.
29. Ono M. Molecular links between tumor angiogenesis and inflammation: inflammatory stimuli of macrophages and cancer cells as targets for therapeutic strategy. Cancer Sci 2008;99:1501–6.
30. Pöld M, Zhu LX, Sharma S, et al. Cyclooxygenase-2-dependent expression of angiogenic CXC chemokines ENA-78/CXC ligand (CXCL) 5 and interleukin-8/CXCL8 in human non-small cell lung cancer. Cancer Res 2004;64:1853–60.
31. Mestas J, Burdick MD, Reckamp K, Pantuck A, Figlin RA, Strieter RM. The role of CXCR2/CXCR2 ligand biological axis in renal cell carcinoma. J Immunol 2005;175:5351–7.
32. Wente MN, Keane MP, Burdick MD, et al. Blockade of the chemokine receptor CXCR2 inhibits pancreatic cancer cell-induced angiogenesis. Cancer Lett 2006;241:221–7.
33. Miyazaki H, Patel V, Wang H, Edmunds RK, Gutkind JS, Yeudall WA. Down-regulation of CXCL5 inhibits squamous carcinogenesis. Cancer Res 2006;66:4279–84.
34. Zhang Z, Rigas B. NF-κB, inflammation and pancreatic carcinogenesis: NF-κB as a chemoprevention target. Int J Oncol 2006;29:185–92.
35. Fujioka S, Sclabas GM, Schmidt C, et al. Inhibition of constitutive NF-κB activity by IκBαM suppresses tumorigenesis. Oncogene 2003;22:1365–70.
36. Greten FR, Eckmann L, Greten TF, et al. IKKβ links inflammation and tumorigenesis in a mouse model of colitis-associated cancer. Cell 2004;118:285–96.
37. Bingle L, Brown NJ, Lewis CE. The role of tumor-associated macrophages in tumor progression: implications for new anticancer therapies. J Pathol 2002;196:254–65.
38. Chen JJ, Yao PL, Yuan A, et al. Up-regulation of tumor interleukin-8 expression by infiltrating macrophages: its correlation with tumor angiogenesis and patient survival in non-small cell lung cancer. Clin Cancer Res 2003;9:729–37.

Overexpression of Class III β-Tubulin Predicts Good Response to Taxane-Based Chemotherapy in Ovarian Clear Cell Adenocarcinoma

Daisuke Aoki,[1] Yoshinao Oda,[3] Satoshi Hattori,[8] Ken-ichi Taguchi,[7] Yoshihiro Ohishi,[3] Yuji Basaki,[5,6] Shinji Oie,[2] Nao Suzuki,[10] Suminori Kono,[4] Masazumi Tsuneyoshi,[3] Mayumi Ono,[5,6] Takashi Yanagawa,[8] and Michihiko Kuwano[6,9]

Abstract **Purpose:** Of the various microtubule-associated molecules, β-tubulin III has been reported to be closely associated with the therapeutic efficacy of taxane-based chemotherapy against ovarian cancer. Stathmin and microtubule-associated protein 4 (MAP4) have been reported to play an important role in microtubule stabilization. In this study, we investigated whether expression of these microtubule-associated factors affects the therapeutic efficacy of taxane-based chemotherapy in ovarian clear cell adenocarcinoma.

Experimental Design: Drug sensitivity of paclitaxel or cisplatin was assessed in ovarian cancer cell lines treated with small interfering RNA of tubulin isoforms, MAP4, and stathmin. We examined 94 surgically resected ovarian clear cell adenocarcinoma specimens from patients treated with taxane-containing regimens ($n = 44$) and with taxane-free regimens ($n = 50$), using immunohistochemistry to detect expression of β-tubulin III, stathmin, and MAP4.

Results: Knockdown of β-tubulin III and IV specifically conferred drug resistance to paclitaxel in one ovarian cancer cell line, but not to other molecules. Estimated overall survival revealed a significant synergistic effect between taxane and β-tubulin III in patients with ovarian clear cell adenocarcinoma. Of three microtubule-related molecules, among the taxane-based chemotherapy group, cases with higher β-tubulin III expression were associated with a significantly more favorable prognosis compared with those having lower β-tubulin III expression. By contrast, there was no statistical significance in the synergistic relationships between stathmin and taxane or between MAP4 and taxane.

Conclusions: Taxane-based chemotherapy was effective for patients with ovarian clear cell adenocarcinomas who were positive for β-tubulin III but not for those who were negative for these proteins.

Microtubules are the principal target of a large and diverse group of natural-product anticancer therapeutic drugs, particularly of two major classes of antimicrotubule agents: the vinca alkaloids and the taxanes (1). Microtubules are composed of polymers of heterodimers that consist of two closely related polypeptides, α-tubulin and β-tubulin, which in turn contain α- or β-subunits and at least six isotypes encoded by different genes. Isotype composition influences the intrinsic dynamics of microtubules, and the sensitivity of microtubules to depolymerizing and polymerizing agents is related to the composition of tubulin isotypes or microtubule-associated proteins (MAP; ref. 2). MAPs, important components of the tubulin and microtubule system, can bind to the microtubule wall and stabilize microtubules (3). MAP2 and MAP-τ are abundantly expressed in mature neurons, and MAP4 is ubiquitously expressed in both proliferating and differentiated cells (4). Stathmin is also the founding member of the microtubule-destabilizing family of proteins, which regulate the dynamics of microtubule polymerization and depolymerization. Stathmin is expressed at high levels in a variety of human cancers

Authors' Affiliations: [1]Department of Obstetrics and Gynecology, School of Medicine, Keio University, and [2]Personalized Medicine Research Laboratory, Taiho Pharmaceutical Co Ltd., Tokyo, Japan; Departments of [3]Anatomic Pathology and [4]Preventive Medicine, Graduate School of Medical Sciences, [5]Department of Pharmaceutical Oncology, Graduate School of Pharmaceutical Sciences, and [6]Innovation Center for Medical Redox Navigation, Kyushu University, and [7]Kyushu National Cancer Center, Fukuoka, Japan; [8]Biostatistics Center and [9]Research Center for Innovative Cancer Therapy, Kurume University, Kurume City, Japan; and [10]Department of Obstetrics and Gynecology, School of Medicine, Saint. Marianna University, Kawasaki, Japan

Received 8/16/08; revised 10/31/08; accepted 11/7/08.

Grant support: Grant-in-Aid for Scientific Research on Priority Areas, Cancer, from the Ministry of Education, Culture, Sports, Science and Technology of Japan (M. Ono), and by the Third Term Comprehensive Control Research for Cancer from the Ministry of Health, Labor and Welfare, Japan (M. Kuwano). This study was also supported, in part, by the Formation of Innovation Center for Fusion of Advanced Technologies, Kyushu University, Japan (M. Ono, Y. Basaki, and M. Kuwano).

The costs of publication of this article were defrayed in part by the payment of page charges. This article must therefore be hereby marked *advertisement* in accordance with 18 U.S.C. Section 1734 solely to indicate this fact.

Note: Supplementary data for this article are available at Clinical Cancer Research Online (http://clincancerres.aacrjournals.org/).

D. Aoki, Y. Oda, S. Hattori, K. Taguchi, Y. Ohishi, and Y. Basaki contributed equally to this work.

Requests for reprints: Daisuke Aoki, Department of Obstetrics and Gynecology, School of Medicine, Keio University, 35 Shinanomachi, Shinjuku-ku, Tokyo 160-8582, Japan. Phone: 81-3-3353-1211; Fax: 81-3-3226-1667; E-mail: aoki@sc.itc.keio.ac.jp.

doi:10.1158/1078-0432.CCR-08-1274

Translational Relevance

It has been reported that β-tubulin III, one of microtubule-associated molecules, was expected to be a useful biomarker for the clinical efficacy of taxane-based chemotherapy against human ovarian cancer. These studies have been conducted in serous adenocarcinoma of ovarian cancer. Previous reports show, however, that ovarian clear cell adenocarcinoma constituted about 20% of ovarian adenocarcinoma in Japan, although only 2% to 5% of cases of ovarian cancer worldwide were clear cell adenocarcinoma. Clear cell adenocarcinoma, which is a rare variant in western counties, has been recognized as a chemoresistant phenotype compared with serous adenocarcinoma, which is the most widespread ovarian cancer. This study aimed to identify a predictive marker for the clinical efficacy of taxane-based chemotherapy against ovarian clear cell adenocarcinoma. In this study, we found that a taxane-based regimen was effective for patients with ovarian clear cell adenocarcinomas who were positive for stathmin or β-tubulin III.

and also plays a role in altered drug sensitivity in human cancer cells, including ovarian cancer cells (5, 6).

The antitumor drug taxane stabilizes microtubules and reduces their dynamics, promoting mitotic arrest and cell death. Paclitaxel, a representative anticancer agent of the taxanes, was initially defined by Horowitz and colleagues, and its binding sites are distinct from those of colchicine, podophyllotoxin, and the vinca alkaloids (7, 8). Paclitaxel initially received regulatory approval for the treatment of patients with ovarian cancer after failure of first-line or subsequent chemotherapy (9). In a Gynecologic Oncology Group study (GOG-111), it was thus determined to be the primary induction therapy in suboptimally debulked stage III and IV ovarian cancer, which mainly consists of serous adenocarcinoma (10). This study first compared the therapeutic efficacy of paclitaxel/cisplatin and cyclophosphamide/cisplatin in patients with ovarian cancer (10). The paclitaxel arm showed a distinct advantage in terms of progression-free survival (PFS) as well as overall survival (OS). A clinical trial by the European Organization for Research and Treatment of Cancer and the National Cancer Institute of Canada also showed that a paclitaxel/cisplatin regimen improved both PFS and OS (11). Another clinical trial study, however, reported that survival in the paclitaxel arm was similar to that seen in the control arm that received either carboplatin or cisplatin, doxorubicin, and cyclophosphamide (12). It remains unclear whether paclitaxel-cisplatin (or carboplatin) therapy is superior to cyclophosphamide/cisplatin (or carboplatin) therapy.

Of the various molecular markers related to drug sensitivity to taxanes, class III β-tubulin is expected to be a useful biomarker for the clinical efficacy of paclitaxel-based chemotherapy. Class III β-tubulin is hypothesized to counteract suppression of microtubule dynamics (13). Ferlini et al. reported that a novel taxane targeting class III β-tubulin overcame paclitaxel resistance, suggesting close involvement of this tubulin isotype in drug sensitivity to paclitaxel (14). Mozzetti et al. reported that class III β-tubulin overexpression represented a prominent mechanism of resistance to paclitaxel-platinum treatment in ovarian cancer (15). Moreover, class III β-tubulin overexpression could be useful in identifying poor clinical outcome in patients with advanced ovarian cancer who are treated with platinum/paclitaxel, those mainly affected with serous adenocarcinoma (16). These studies have been conducted mainly in serous adenocarcinoma of ovarian cancer. It remains unknown, however, whether class III β-tubulin overexpression is also predictive of poor outcome in clear cell adenocarcinoma, which is a rare variant in western countries, where it is reported to constitute 5% to 10% of ovarian carcinomas (17–19). Clear cell adenocarcinoma has been recognized as a chemoresistant phenotype (20, 21).

Japanese investigators have reported that clear cell adenocarcinoma constitutes about 20% of ovarian carcinomas in Japan (20, 22), although clear cell adenocarcinoma of the ovary accounts for only 2% to 5% of cases enrolled in large-scale randomized trials worldwide (22, 23). Thus, it is unclear whether carboplatin/paclitaxel therapy, which was introduced broadly as a standard regimen for epithelial ovarian cancer based on the results of such trials, can be readily applied for clear cell adenocarcinoma. Development of novel treatment strategies based on molecular biological characteristics is further required for clear cell adenocarcinoma.

In the present study, we addressed whether expression of β-tubulin III, MAP4, and stathmin could affect the efficacy of taxane-based therapeutic regimens against clear cell adenocarcinoma. Using immunohistochemical analysis of surgically resected clinical samples of clear cell adenocarcinoma, we examined expression levels of the above three biomarkers. In comparison with ovarian cancer patients treated with taxane-free regimens, we observed a significant and specific association of β-tubulin III expression with therapeutic outcomes of ovarian cancer treated with taxane-based regimens. We discuss whether the expression of β-tubulin III could be a predictive marker for the clinical efficacy of taxane-based chemotherapy against ovarian clear cell adenocarcinoma.

Materials and Methods

Cells and reagents. The human ovarian cell lines OVCAR-3 and SKOV-3, which expressed β-tubulins (I, II, III, and IV), MAP4, and stathmin, were obtained from the American Type Culture Collection. Cells were grown in Ham's F-12 Medium (Nissui Seiyaku Co.) with 10% fetal bovine serum (FetalClone III; Hyclone), 100 IU/mL penicillin, and 100 μg/mL streptomycin (Life Technologies, Inc.) in a humidified atmosphere of 5% CO_2 at 37°C. Paclitaxel (Taxol injection) and cisplatin (Briplatin injection) purchased from Bristol-Myers Squibb were clinically used. The polyclonal antistathmin was obtained from Calbiochem. The monoclonal class III β-tubulin antibody (clone 5G8) was obtained from Promega. The monoclonal MAP4 antibody (clone 18) was purchased from BD Transduction Laboratories.

Silencing of β-tubulins (I, II, III, IV), MAP4, and stathmin genes. To reduce the expression of some genes, we used Stealth RNAi (Invitrogen Life Technologies) to knock down the expression of β-tubulin I (NM_030773_stealth_706), β-tubulin II (NM_001069_stealth_1444), β-tubulin III (NM_006086_stealth_233), β-tubulin IV (NM_006087_stealth_352), MAP4 (NM_002375_stealth_2042), and stathmin (STMN1-HSS142799). Subconfluent human ovarian cells were cultured overnight in Opti-MEM I medium (Invitrogen Life

Technologies) without antibiotics, then 40 nmol/L small interfering RNA (siRNA) and Lipofectamine RNAiMax (Invitrogen) were applied according to the manufacturer's instructions. After 32 h, cells were detached from the culture plates and seeded into 96-well plates in F-12 medium with 10% fetal bovine serum. After a further 16-h incubation, paclitaxel or cisplatin was applied and cells were cultured for 3 d more. The numbers of cells were estimated by WST-8. The IC_{50} value was estimated from the regression line of log-logit plots of T/C (%) value versus drug concentration. The assays were carried out in quadruplicate.

Quantitative real-time PCR. RNA was reverse-transcribed from random hexamers using AMV reverse transcriptase (Promega). Real-time quantitative PCR was done using the Real-Time PCR system 7300 (Applied Biosystems). In brief, the PCR amplification reaction mixtures (20 μL) contained cDNA, primer pairs, the dual-labeled fluorogenic probe, and TaqMan Universal PCR Master Mix (Applied Biosystems). The thermal cycle conditions included maintaining the reactions at 50°C for 2 min and at 95°C for 10 min, and then alternating for 40 cycles between 95°C for 15 s and 60°C for 1 min. The primer pairs and probes were obtained from Applied Biosystems. The relative gene expression for each sample was determined using the formula $2^{(-\text{delta Ct})} = 2^{(\text{Ct (GAPDH)-Ct (target)})}$, which reflected the target gene expression normalized to GAPDH levels.

Patients. Ninety-four patients with primary ovarian clear cell adenocarcinoma, who had undergone debulking surgery at Keio University Hospital from 1983 to 2005, were examined. The histopathologic diagnoses of the all cases were confirmed according to the most recent WHO classification (WHO 2003). Patients were staged according to the International Federation of Obstetrics and Gynecology (FIGO) classification (24). Forty-four patients underwent chemotherapy using regimens containing taxanes [paclitaxel plus carboplatin (n = 39), paclitaxel plus cisplatin (n = 3), docetaxel plus cisplatin (n = 2); paclitaxel, 180 mg/m^2 body surface/day 1, docetaxel, 70 mg/m^2 body surface/day 1, cisplatin, 60 mg/m^2 body surface/day 1, and carboplatin, area under the curve 6/day 1]. Fifty patients received taxane-free regimens [CAP groups (n = 36): cisplatin (60 mg/m^2 body surface/day 1), epirubicin (50 mg/m2 body surface/day 1), and cyclophosphamide (500 mg/m^2 body surface/day 1); CAP plus fluorouracil (n = 1), CAP plus tegafur-uracil (n = 2), cisplatin plus cyclophosphamide (n = 11)]. The doses of carboplatin were calculated using Calvert's formula.

The effect of chemotherapy was evaluated approximately every 6 mo by computed tomography after 6 cycles of administration of chemotherapy. After chemotherapy, all patients were followed up every 2 mo for the first year, every 3 to 4 mo for the next 2 y, and every 6 mo

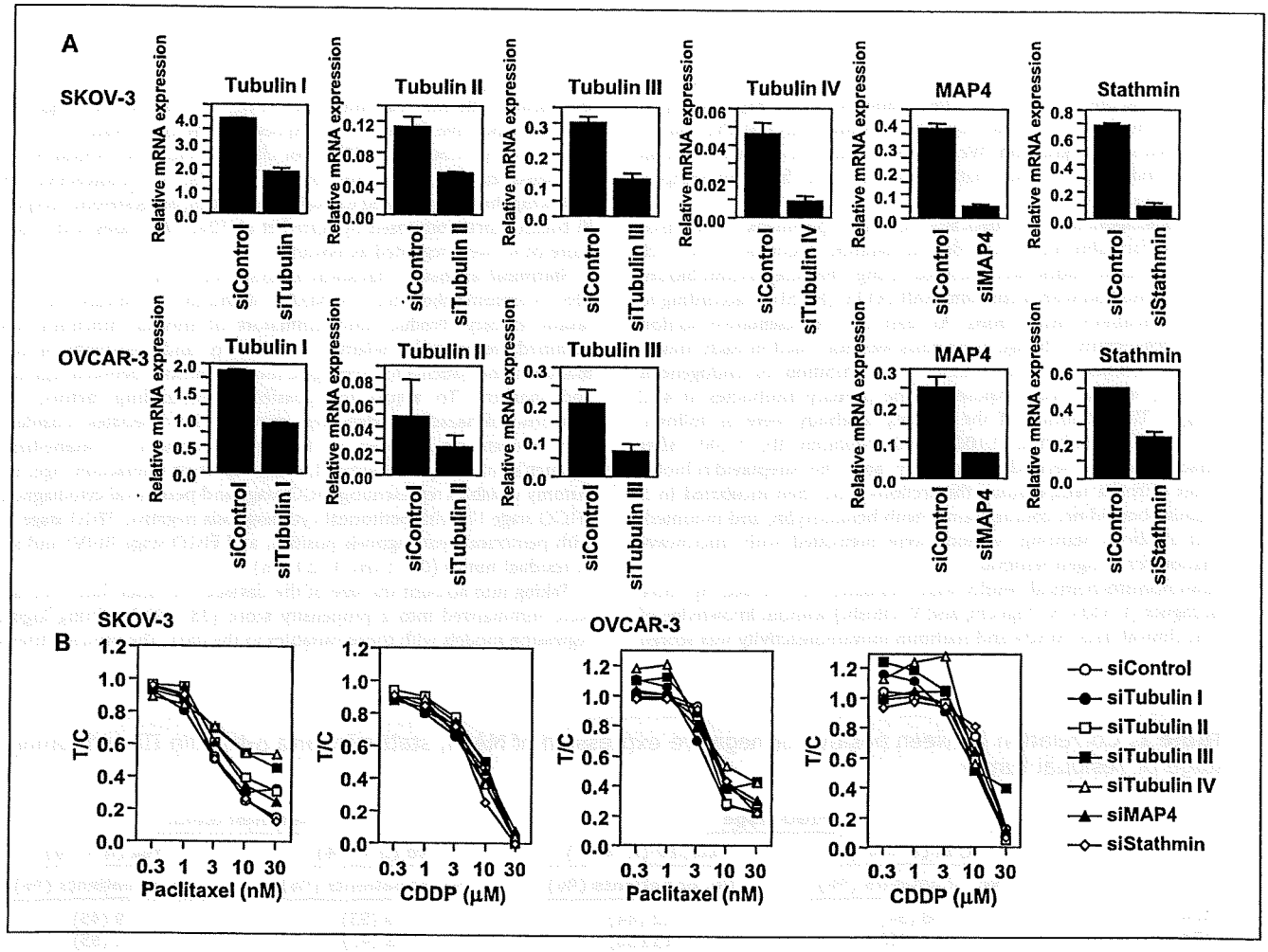

Fig. 1. Drug sensitivity to paclitaxel or cisplatin in human ovarian cancer cells treated with siRNA for β-tubulin isoforms, MAP4, and stathmin. *A*, mRNA expression of β-tubulin isoforms (I, II, III, IV), MAP4, and stathmin after treatment with respective siRNA for 48 h were determined by real-time PCR analysis. The expression of β-tubulin IV mRNA in OVCAR-3 cells was not detected. *B*, cells treated with respective siRNA were seeded into 96-well plates at 2 × 10^3 cells/0.1 mL/well and incubated overnight. On the following day, a 100-μL aliquot containing paclitaxel or cisplatin was added to the wells and cultured for a further 3 d. The number of viable cells was estimated using the WST-8 assay. The assays were carried out in quadruplicate.

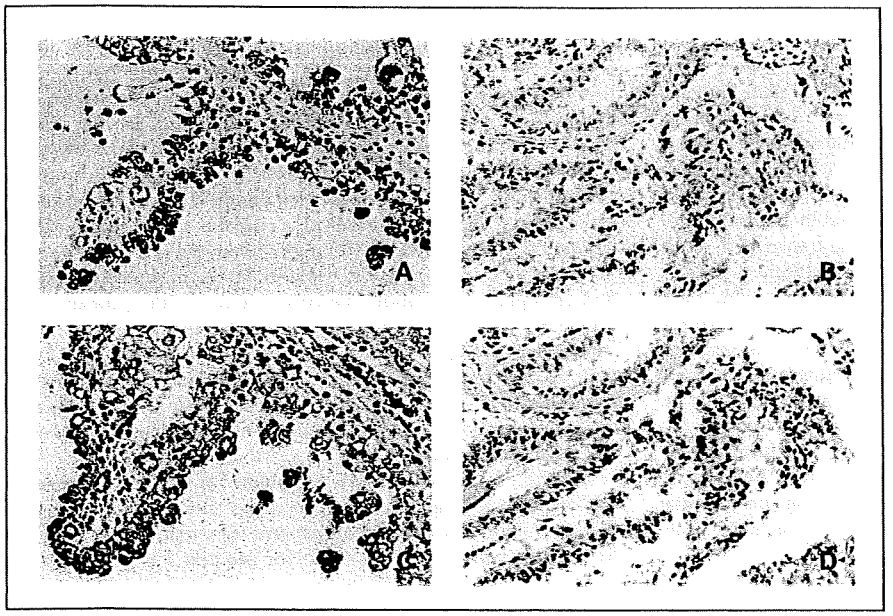

Fig. 2. *A* and *C*, stage IIc clear cell adenocarcinoma of a 55-year-old woman treated with the paclitaxel-carboplatin regimen. Cytoplasmic strong expression of stathmin (*A*, >15%) and β-tubulin III (*C*, score 7) can be diffusely observed in the tumor cells. The patient currently shows no evidence of disease 2,487 d (83 mo) after surgery. *B* and *D*, stage IIc tumor of a 56-year-old woman treated with the paclitaxel-carboplatin regimen. A few tumor cells (<15%) show only faint immunoreactivity for stathmin in the cytoplasm or nuclei, which was judged as negative (*C*). β-Tubulin III can be recognized in 10% of tumor cells with intermediate intensity and was interpreted as negative (score 4; *D*). This patient died of disease 447 d (15 mo) after initial surgery.

thereafter. Clinical outcome was measured by PFS and OS. PFS was defined as the interval from the date of first treatment (laparotomy or the first administration of neoadjuvant chemotherapy) to the date of the diagnosis of progression. We obtained informed consent from all patients, and personal information was removed from all samples before analysis.

Immunohistochemistry. Surgically resected specimens were fixed with 10% formalin and embedded in paraffin. Sections 4-μm thick on silane-coated slides were stained using the streptavidin-biotin-peroxidase method with a Histofine SAB-PO kit (Nichirei) according to the manufacturer's instructions. At least one representative section without degenerative change or necrosis was examined in each tumor. After deparaffinization, rehydration, and inhibition of endogenous peroxidase, sections were exposed to the primary antibodies at 4°C overnight. The dilutions of the primary antibody were as follows: MAP4, 1:1500; stathmin, 1:1000; and β-tubulin III, 1:200. After incubation of the secondary antibody and the streptavidin-biotin complex at room temperature, the sections were then incubated in 3 3′- diaminobenzidine, counterstained with hematoxylin, and mounted. For all antibody staining, sections were pretreated with microwave irradiation for antigen retrieval.

Immunohistochemical results were evaluated and scored by three pathologists (Y. Oda, K. Taguchi, and Y. Ohishi) without knowledge of patient clinical data. MAP4 and stathmin immunoreactivity was scored by estimating the percentage of labeled tumor cells. When >80% of the tumor cells showed immunoreactivity for MAP4, we judged the case to be positive. For stathmin expression, the cutoff value was 15%, based on a previous study (25). For class III β-tubulin expression, we evaluated the proportion and intensity of the immunoreactive cells following the protocol used to evaluate estrogen/progesterone receptors in breast cancer, proposed by Allred et al. (26, 27). Cases with a total score of =7 were regarded as positive.

Statistical analysis. Statistical analysis was conducted for OS and PFS to examine the effects of MAP4, stathmin, and β-tubulin III on taxane efficacy. Product-limit estimators of survival functions were obtained, respectively, relative to positivity and negativity of each marker in the patients to investigate the relationship between regimens and markers. To adjust for possible confounding factors, Cox proportional hazards models were applied. The covariates considered were a treatment indicator (0, taxane-free regimen; 1, taxane-based regimen), marker (0, negative; 1, positive), their interaction, age, two dummy variables representing FIGO stage and peritoneal cytodiagnosis (FIGO stage I-II with peritoneal cytodiagnosis negative, FIGO stage I-II with peritoneal cytodiagnosis positive, and FIGO stage III-IV) and size of residual tumor (0, <1 cm; 1, ≥1 cm).

Taking into account the size of the dataset, the latter four covariates were summarized into a propensity score (28, 29) by fitting logistic regression models with those variables to the data. The primary interest

Table 1. Correlation between positive or negative expression of MAP4, stathmin, and β-tubulin III and tumor stage or residual tumor

	FIGO stage		Residual tumor	
	I/II (*n* = 67)	III/IV (*n* = 27)	No (*n* = 74)	Yes (*n* = 20)
	No. of patients (%)	No. of patients (%)	No. of patients (%)	No. of patients (%)
MAP4 (-)	36 (54)	12 (44)	39 (53)	9 (45)
MAP4 (+)	31 (46)	15 (56)	35 (47)	11 (55)
Stathmin (-)	29 (43)	11 (41)	33 (45)	7 (35)
Stathmin (+)	38 (57)	16 (59)	41 (55)	13 (65)
β-tubulin III (-)	30 (45)	11 (41)	33 (45)	8 (40)
β-tubulin III (+)	37 (45)	16 (59)	41 (55)	12 (60)

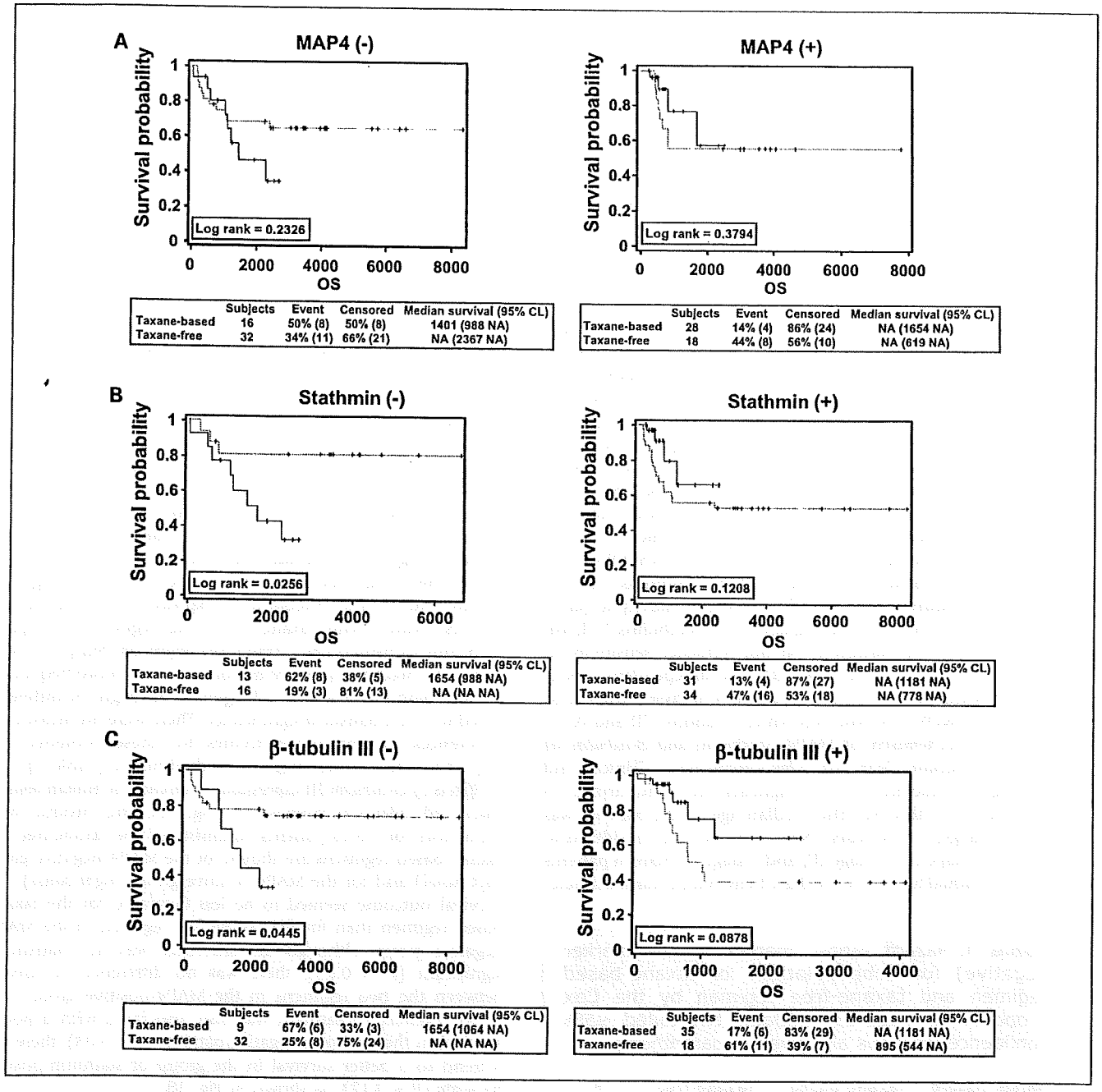

Fig. 3. The product-limit estimator of OS by regimens and microtubule-associated molecules. *A*, the product-limit estimators of OS for MAP4-negative patients (*left panel*) and for positive patients (*right panel*). *B*, the product-limit estimators of OS for stathmin-negative patients (*left panel*) and for positive patients (*right panel*). *C*, the product-limit estimators of OSfor β-tubulin III negative patients (*left panel*) and for positive patients (*right panel*). Solid lines, survival functions of patients receiving the taxane-based regimen; broken line, taxane-free regimen.

was the effect of the interaction between treatment and marker. With the supposition that the effect of a taxane-based regimen for marker-negative patients equals *A* and that of the taxane-free regimen for positive patients equals *B*, the significance of the interaction shows that the effect of the taxane-based regimen for the marker-positive patients is greater than *A+B* (i.e., it is synergistic). Evidence of a synergistic effect indicates that the effect of taxane is dependent on the status of the marker, showing the marker plays an important role in the effect of taxane. The cutoff points that determined positive and negative for each marker were chosen by the Akaike's information criterion so that the Cox model fitted best to the data (30).

Results

Effects of reducing expression of β-tubulin isoforms, MAP4, and stathmin on drug sensitivity to paclitaxel and cisplatin in ovarian cancer cells. We first examined whether gene silencing of

Table 2. Summary of interaction terms for the Cox regression

	MAP4	Stathmin	β-tubulin III
OS			
Regression coefficient (95% CI)	-0.77 (-2.50 to 0.96)	-1.37 (-3.17 to 0.43)	-1.68 (-3.16 to 0.21)
P	0.383	0.135	0.026
PFS			
Regression coefficient (95% CI)	-0.40 (-1.91 to 1.12)	-0.85 (-2.43 to 0.72)	-1.52 (-2.90 to -0.15)
P	0.608	0.288	0.030

Abbreviation: 95% CI, 95% confidence interval.

β-tubulin isoforms, MAP4, and stathmin could affect drug sensitivity to paclitaxel and cisplatin in the cultured human ovarian cancer cell lines SKOV-3 and OVCAR-3. Cellular mRNA expression levels of these genes in two human ovarian cancer cell lines were all markedly down-regulated when treated with respective siRNA (Fig. 1A). We then examined the drug sensitivities of paclitaxel or cisplatin in ovarian cancer cells treated with siRNA of the tubulin isoforms, MAP4, and stathmin (Fig. 1B). When β-tubulin III or β-tubulin IV was silenced, the IC_{50} values of paclitaxel increased to 16.8 nmol/L and 14.3 nmol/L, respectively, from the control IC_{50} value of 3.9 nmol/L in SKOV-3 cells (Fig. 1B). By contrast, down-regulation of β-tubulins I and II, MAP4, and stathmin did not influence the sensitivity to paclitaxel in SKOV-3 cells. Down-regulation of β-tubulins I, II, III, and IV, MAP4, and stathmin did not influence sensitivity to cisplatin in either cell line (Fig. 1B). Two independent experiments consistently showed the acquisition of drug resistance to paclitaxel in SKOV-3 by knockdown of β-tubulins III and IV.

Immunohistochemistry of MAP4, stathmin, and β-tubulin III in human ovarian clear cell adenocarcinomas. Clinical and pathologic characteristics at diagnosis are summarized in Supplementary Table S1. The median age of the patients was 52 years (range, 29-74 years). Sixty tumors were considered to be stage I, 7 stage II, 20 stage III, and 7 stage IV. Sixteen patients who had residual tumors more than 1 cm in maximum diameter were classified into the suboptimal group, whereas 78 patients were placed in the optimal group with a residual tumor ≤1 cm, including 74 complete resections. The median follow-up for PFS for all 94 patients was 749 days (range, 23-8,318 days), whereas the median follow-up for OS was 995 days (range, 23-8,318 days). The median follow-up of those patients who are currently progression-free is 2,399 days (range, 212-8,318 days).

Table 3. Hazard ratios (marker positive/marker negative) for subpopulations of taxane-based regimen and taxane-free regimen by the Cox proportional hazards models; two-tailed 95% confidence intervals are given in parenthesis

Marker hazard ratio (95% CI)	Taxane-based therapy	Taxane-free therapy	*P*
Overall survival			
MAP4	0.42 (0.11-1.66)	0.91 (0.35-2.40)	0.383
Stathmin	0.96 (0.26-3.53)	3.78 (1.07-13.34)	0.135
β-tubulin III	0.72 (0.22-2.44)	3.91 (1.49-10.23)	0.026
Progression-free survival			
MAP4	0.53 (0.17 -1.69)	0.79 (0.31-2.02)	0.608
Stathmin	1.11 (0.36-3.41)	2.60 (0.85-7.96)	0.288
β-tubulin III	0.77 (0.26-2.31)	3.52 (1.37-9.01)	0.030

NOTE: Age, FIGO stage, peritoneal cytodianosis, and size of residual tumor were adjusted by the propensity scores representing the four covariates.
P values are based on Wald tests for interaction of taxane with the marker.

The cytoplasmic positive expression of MAP4 was detected in 46 tumors (49%). Positive immunostaining for stathmin was found in 54 tumors (57%), predominantly as cytoplasmic staining (Fig. 2A). β-Tubulin III immunostaining was positive in 53 (56%) tumors with total scores of 7 or 8 (Fig. 2C). Positive MAP4 and β-tubulin III expression was frequent in tumors treated with taxane-containing regimens, compared with tumors treated with taxane-free regimens (Supplementary Table S1). Stathmin-positive tumors were also more frequent in patients with the taxane-based regimen, although the difference failed to reach statistical significance. There were no measurable differences in immunoreactivities for these proteins with respect to either tumor stage or residual tumor (Table 1).

Effects of β-tubulin III expression on survival in human ovarian clear cell adenocarcinomas. In Fig. 3A, the product-limit estimators for OS of patients administered the taxane-free and taxane-based regimens are shown for the MAP4-negative group (*left panel*) and for the MAP4-positive group (*right panel*). The survival outcome seemed to be less favorable for the taxane-based regimen than for the taxane-free regimen in the MAP4-negative group, although the difference was not statistically significant ($P = 0.23$); there was no difference in survival between the two regimens in the MAP4-positive group ($P = 0.38$). Paclitaxel treatment was also associated with a poorer survival in the stathmin-negative patients ($P = 0.03$); there was a trend to a better survival in the group of stathmin-positive patients ($P = 0.12$), as shown in Fig. 3B.

Survival associated with paclitaxel treatment was more evidently differential based on β-tubulin III status. In the absence of β-tubulin III expression, survival was significantly shorter in patients with the taxane-based regimen compared with those with the taxane-free regimen ($P = 0.04$), and the opposite was the case in the presence of β-tubulin III expression ($P = 0.09$; Fig. 3C). Table 2 gives the estimates, confidence intervals, and *P* values for the hazard ratios of the interaction. The table shows that for β-tubulin III, *P* values were 0.026 for OS and 0.030 for PFS. Thus, β-tubulin III seems to determine the efficacy of the taxane-based regimen. Table 2 also shows that for stathmin, *P* was 0.135 and the hazard ratio was 0.25 (95% confidence interval, 0.04-1.53) for OS, and 0.288 and 0.43, respectively (95% confidence interval, 0.09-2.06), for PFS.

Thus, stathmin may also determine the efficacy of the taxane-based regimen, but the effect was not statistically significant. Furthermore, Table 2 shows that for MAP4, the estimated hazard ratios were far from 1 but were not statistically significant (0.383 for OS and 0.673 for PFS).

The statistical significance of the interaction of taxane with β-tubulin III shown in Table 2 indicates that the efficacy of taxane depends on β-tubulin III positivity or negativity. To interpret this interaction precisely, we give the hazard ratio of the taxane-based regimen relative to the taxane-free regimen separately for β-tubulin III–positive and -negative patients. Table 3 gives the hazard ratios for patients who were positive for β-tubulin III relative to patients who were negative; these ratios are given separately for the taxane-based and taxane-free regimens. The table shows that the hazard ratio for OS was 3.91 for the taxane-free regimen but was 0.72 for the taxane-based regimen. This outcome indicates that being positive for β-tubulin III is related to a poor prognosis in the taxane-free regimen group, but that the taxane-based regimen may prolong OS for patients who are β-tubulin III–positive.

Discussion

Class III β-tubulin overexpression has been reported to be a marker of poor clinical outcome in patients with advanced ovarian cancer mainly containing serous type adenocarcinoma. With treatment using platinum/paclitaxel therapy (16), expression of class III β-tubulin also predicts response and outcome in patients with non–small cell lung cancer and in those with breast cancer who are treated with taxane-based chemotherapy (31, 32). In this study, we investigated which targets could be responsible for the therapeutic efficacy of taxane-based chemotherapy against ovarian clear cell adenocarcinoma patients when treated with either cisplatin/cyclophosphamide or cisplatin/taxane. Immunohistochemical staining was done for the surgically resected specimens using antibodies against class III β-tubulin, MAP4, and stathmin. Of these three targeting molecules, expression of class III β-tubulin was significantly associated with therapeutic efficacy of taxane-based chemotherapy, but not with taxane-free chemotherapy. Moreover, our present study showed that increased expression of class III β-tubulin significantly affected outcome for patients with ovarian clear cell adenocarcinoma in the taxane-treated patient group.

Our present finding is not consistent with those of previous studies identifying a close association of class III β-tubulin overexpression with poor therapeutic efficacy of taxane-based chemotherapy against ovarian cancers, including most non–clear cell adenocarcinomas (14–16). Of β-tubulin isoforms, microtubules containing tubulin III or IV were more dynamic and less stable than microtubules containing other tubulin types (13, 33), suggesting that cellular expression of β-tubulin isotype III or IV plays a critical role in drug sensitivity to paclitaxel *in vitro*. Paclitaxel-selected drug-resistant cancer cell lines derived from human lung, breast, pancreas, and prostate cancers and glioblastoma often exhibit enhanced expression of β-tubulin III (34). Kavallaris et al. have previously reported increased mRNA expression of β-tubulins III and IV in taxane-treated ovarian tumor samples as compared with primary untreated ovarian tumors (35). However, Nicolletti et al. have reported no correlation between tubulin expression and paclitaxel sensitivity in mouse xenografts of human ovarian carcinomas (36).

In our present study, knockdown of class III and IV β-tubulin genes but not of other tubulin isoforms specifically decreased drug sensitivity to paclitaxel in one ovarian cancer cell line, indicating the possible involvement of these tubulin isoforms in the dynamics of microtubules. At present, it remains unclear why decreased expression of type III β-tubulin differentially modulates drug sensitivity to paclitaxel among various cancer cell lines *in vitro*, and this finding requires further study. A complex network system among microtubule-related factors, including tubulin isoforms, operates in limiting drug sensitivity to taxanes; however, the results of our present study together with those of previous reports could present a novel notion that expression levels of class III β-tubulin might thus predict the therapeutic efficacy of taxane-based therapy. This effect would depend on differences in pathologic subtype between serous adenocarcinoma and clear cell adenocarcinoma.

We also found that OS of patients with lower expression of MAP4, stathmin, and β-tubulin indicated better therapeutic efficacy with non–taxane-based chemotherapy compared with taxane-based treatment. In patients with higher expression of stathmin and MAP4, these relationships were reversed but not statistically significant. Although these appeared during follow-up periods of the taxane-based therapy group for as long as 3,000 days, low expression of these three targeting molecules might predict poor prognosis for patients with ovarian clear cell adenocarcinoma.

Altered expression of proteins that regulate microtubule dynamics also mediates paclitaxel resistance in cancer cells *in vitro* through interaction with tubulin dimers or polymerizing microtubules. These proteins include stathmin, a microtubule destabilizer, and MAP4, a microtubule stabilizer (34). Altered expression of stathmin (5, 6) and MAP-4 (37) induces marked changes in drug sensitivity of cancer cells to taxanes. Further study is required to understand whether the above mechanisms *in vitro* underlie the poor therapeutic efficacy of taxane-based chemotherapy for patients with low expression of stathmin and MAP4, as well as β-tubulin. On the other hand, increased expression of stathmin also was associated (but not significantly) with an improved therapeutic efficacy of taxane-based chemotherapy in comparison with that of taxane-free therapy. Further study with a larger number of patients as well as longer follow-up periods may predict whether stathmin can be a marker for therapeutic efficacy of taxane-based therapy against ovarian clear cell adenocarcinoma.

In conclusion, our present study showed that overexpression of type III β-tubulin was a predictive marker of better prognosis for patients with ovarian clear cell adenocarcinoma when they are treated with taxane-based chemotherapy. This finding is not consistent with those involving patients with other serous type carcinoma treated by taxane-based chemotherapy, suggesting that association of β-tubulin expression with therapeutic efficacy by taxane-based chemotherapy depends on the pathologic characteristics of ovarian cancer.

Disclosure of Potential Conflicts of Interest

No potential conflicts of interest were disclosed.

References

1. Jordan MA. Mechanism of action of antitumor drugs that interact with microtubules and tubulin. Curr Med Chem Anti-Canc Agents 2002;2:1–17.
2. Drukman S, Kavallaris M. Microtubule alterations and resistance to tubulin-binding agents. Int J Oncol 2002; 21:621–8.
3. Maccioni RB, Cambiazo V. Role of microtubule-associated proteins in the control of microtubule assembly. Physiol Rev 1995;75:835–64.
4. Chapin SJ, Lue CM, Yu MT, Bulinski JC. Differential expression of alternatively spliced forms of MAP4: a repertoire of structurally different microtubule-binding domains. Biochemistry 1995;34:2289–301.
5. Balachandran R, Welsh MJ, Day BW. Altered levels and regulation of stathmin in paclitaxel-resistant ovarian cancer cells. Oncogene 2003;22:8924–30.
6. Alli E, Bash-Babula J, Yang JM, Hait WN. Effect of stathmin on the sensitivity to antimicrotubule drugs in human breast cancer. Cancer Res 2002;62: 6864–9.
7. Schiff PB, Fant J, Horwitz SB. Promotion of microtubule assembly *in vitro* by taxol. Nature 1979;277: 665–7.
8. Manfredi JJ, Parness J, Horwitz SB. Taxol binds to cellular microtubules. J Cell Biol 1982;94:688–96.
9. Rowinsky EK, Donehower RC. Paclitaxel (taxol). N Engl J Med 1995;332:1004–14.
10. McGuire WP, Hoskins WJ, Brady MF, et al. Cyclophosphamide and cisplatin compared with paclitaxel and cisplatin in patients in patients with stage III and stage IV ovarian cancer. N Engl J Med 1996;334:1–6.
11. Piccart MJ, Bertelsen K, James K, et al. Randomized intergroup trial of cisplatin-paclitaxel versus cisplatin-cyclophosphamide in women with advanced epithelial ovarian cancer: three-year results. J Natl Cancer Inst 2000;92:699–708.
12. International Collaborative Ovarian Neoplasm Group. Paclitaxel plus carboplatin versus standard chemotherapy with either single-agent carboplatin or cyclophosphamide, doxorubicin, and cisplatin in women with ovarian cancer: the ICON3 randomised trial. Lancet 2002;360:505–15.
13. Derry WB, Wilson L, Khan IA, Luduena RF, Jordan MA. Taxol differentially modulates the dynamics of microtubules assembled from unfractionated and purified β-tubulin isotypes. Biochemistry 1997;36: 3554–62.
14. Ferlini C, Raspaglio G, Mozzetti S, et al. The secotaxane IDN5390 is able to target class III β-tubulin and to overcome paclitaxel resistance. Cancer Res 2005;65:2397–405.
15. Mozzetti S, Ferlini C, Concolino P, et al. Class III β-tubulin overexpression is a prominent mechanism of paclitaxel resistance in ovarian cancer patients. Clin Cancer Res 2005;11:298–305.
16. Ferrandina G, Zannoni GF, Martinelli E, et al. Class III β-tubulin overexpression is a marker of poor clinical outcome in advanced ovarian cancer patients. Clin Cancer Res 2006;12:2774–9.
17. Scully RE. Tumors of the ovary and maldeveloped gonads. 3rd series. Washington (DC): Armed Forced Institute of Pathology; 1996. p. 141.
18. Seidman JD, Russell P, Kurman RJ. Surface epithelial tumors of the ovary. In: Blaustein A, Kurman RJ. Blaustein's pathology of the female genital tract. 5th ed. New York: Springer-Verlag; 2002. p. 873.
19. Shimizu M, Nikaido T, Toki T, Shiozawa T, Fujii S. Clear cell carcinoma has an expression pattern of cell cycle regulatory molecules that is unique among ovarian adenocarcinomas. Cancer 1999;85:669–77.
20. Ozols RF, Bundy BN, Greer BE, et al. Phase III trial of carboplatin and paclitaxel compared with cisplatin and paclitaxel in patients with optimally resected stage III ovarian cancer: a Gynecologic Oncology Group study. J Clin Oncol 2003;21:3194–200.
21. Sugiyama T, Kamura T, Kigawa J, et al. Clinical characteristics of clear cell carcinoma of the ovary. Cancer 2000;88:2584–9.
22. Pectasides D, Fountzilas G, Aravantinos G, et al. Advanced stage clear-cell epithelial ovarian cancer: the Hellenic Cooperative Oncology Group experience. Gynecol Oncol 2006;102:285–91.
23. du Bois A, Lück HJ, Meier W, et al. A randomized clinical trial of cisplatin/paclitaxel versus carboplatin/paclitaxel as first-line treatment of ovarian cancer. J Natl Cancer Inst 2003;95:1320–9.
24. International Federation of Gynecology and Obstetrics. Changes in definitions of clinical staging for cancer of the cervix and ovary. Am J Obstet Gynecol 1987;156:236–41.
25. Yuan RH, Jeng YM, Chen HL, et al. Stathmin overexpression cooperates with p53 mutation and osteopontin overexpression, and is associated with tumour progression, early recurrence, and poor prognosis in hepatocellular carcinoma. J Pathol 2006;209: 549–58.
26. Allred DC, Harvey JM, Berardo M, Clark GM. Prognostic and predictive factors in breast cancer by immunohistochemical analysis. Mod Pathol 1998;11: 155–68.
27. Ohishi Y, Oda Y, Basaki Y, et al. Expression of β-tubulin isotypes in human primary ovarian carcinoma. Gynecol Oncol 2007;105:586–92.
28. Rosenbaum PR, Rubin DB. The central role of the propensity score in observational studies for causal effects. Biometrika 1983;70:41–55.
29. Rosenbaum PR, Rubin DB. Reducing bias in observational studies using subclassification on the propensity score. J Am Stat Assoc 1984;79:516–24.
30. Akaike H. "A new look as the statistical model identification." IEEE Trans Autom Contr 1974;19:716–23.
31. Sève P, Mackey J, Isaac S, et al. Class III β-tubulin expression in tumor cells predicts response and outcome in patients with non-small cell lung cancer receiving paclitaxel. Mol Cancer Ther 2005;4:2001–7.
32. Paradiso A, Mangia A, Chiriatti A, et al. Biomarkers predictive for clinical efficacy of taxol-based chemotherapy in advanced breast cancer. Ann Oncol 2005; 16:14–9.
33. Panda D, Miller HP, Banerjee A, Luduena RF, Wilson L. Microtubule dynamics *in vitro* are regulated by the tubulin isotype composition. Proc Natl Acad Sci U S A 1994;91:11358–62.
34. Orr GA, Verdier-Pinard P, McDaid H, Horwitz SB. Mechanisms of Taxol resistance related to microtubules. Oncogene 2003;22:7280–95.
35. Kavallaris M, Kuo DY, Burkhart CA, et al. Taxol-resistant epithelial ovarian tumors are associated with altered expression of specific β-tubulin isotypes. J Clin Invest 1997;100:1282–93.
36. Nicoletti MI, Valoti G, Giannakakou P, et al. Expression of β-tubulin isotypes in human ovarian carcinoma xenografts and in a sub-panel of human cancer cell lines from the NCI-Anticancer Drug Screen: correlation with sensitivity to microtubule active agents. Clin Cancer Res 2001;7:2912–22.
37. Zhang CC, Yang JM, Bash-Babula J, et al. DNA damage increases sensitivity to vinca alkaloids and decreases sensitivity to taxanes through p53-dependent repression of microtubule-associated protein 4. Cancer Res 1999;59:3663–70.

Bioorganic & Medicinal Chemistry Letters 19 (2009) 3863–3865

Contents lists available at ScienceDirect

Bioorganic & Medicinal Chemistry Letters

journal homepage: www.elsevier.com/locate/bmcl

Total synthesis and determination of the absolute configuration of FD-838, a naturally occurring azaspirobicyclic product

Yujiro Hayashi [a,b,*], Kuppusamy Sankar [a], Hayato Ishikawa [a], Yuriko Nozawa [c], Kazutoshi Mizoue [c], Hideaki Kakeya [d]

[a] Department of Industrial Chemistry, Faculty of Engineering, Tokyo University of Science, Kagurazaka, Shinjuku-ku, Tokyo 162-8601, Japan
[b] Research Institute for Science and Technology, Tokyo University of Science, Kagurazaka, Shinjuku-ku, Tokyo 162-8601, Japan
[c] Research Center of Taisho Pharmaceutical Co., Ltd, 1-403, Yoshino-cho, Kita-ku, Saitama-shi, Saitama 331-9530, Japan
[d] Department of System Chemotherapy and Molecular Sciences, Graduate School of Pharmaceutical Sciences, Kyoto University, Sakyo-ku, Kyoto 606-8501, Japan

ARTICLE INFO

Article history:
Received 5 March 2009
Revised 27 March 2009
Accepted 30 March 2009
Available online 5 April 2009

Keywords:
FD-838
Total synthesis
Absolute configuration

ABSTRACT

The first asymmetric total synthesis of FD-838, a naturally occurring azaspirobicyclic product, has been accomplished allowing determination of its absolute stereochemistry.

Pseurotins,[1] synerazol,[2] and azaspirene[3] are natural products possessing a unique azaspirocyclic framework, such as the 1-oxa-7-azaspiro[4.4]non-2-ene-4,6-dione ring system (Fig. 1). The pseurotins are a small family of secondary microbial metabolites isolated from a culture broth of *Pseudeurotium ovalis* (strain S2269/F) in 1976 by Bloch et al.[1a] Pseurotin A was reported to inhibit chitin synthase by Sterner and co-workers in 1993,[1e] and was also found to induce cell differentiation of PC12 cells by Komagata et al. in 1995.[1f] The structure of pseurotin A, including its absolute stereochemistry, has been unambiguously determined by a single-crystal X-ray analysis of its 12,13-dibromo derivative.[1b] Synerazol, an antifungal antibiotic isolated by Ando and co-workers in 1991 from the culture broth of *Aspergillus fumigatus* SANK 10588, is active against *Candida albicans* and other fungi, showing marked synergistic activity with azole-type antifungal agents.[2] Azaspirene, isolated from the fungus *Neosartorya* sp. by Kakeya and co-workers was found not only to inhibit the endothelial migration induced by vascular endothelial growth factor,[3] but also to exhibit antiangiogenic effects by blocking Raf-1 activation.[4] These compounds possess the same highly oxygenated azaspiro core structure with different side chains. Because of its unique structure and interesting biological properties, there have been several attempts at its total synthesis.[5] Our group has accomplished the first enantioselective total synthesis of pseurotin A,[6] F2,[6] synerazol,[7] and azaspirene,[8] in which the aldol chemistry of a chiral benzylidene lactam with an appropriate aldehyde, followed by successive oxidation and dehydration, creates the key azaspiro structure (Eq. 1). By these syntheses, the absolute configurations of synerazol[9] and azaspirene have been determined. Tadano and co-workers also reported the total syntheses of pseurotin A, F2, and azaspirene from D-glucose.[10]

FD-838, isolated from *A. fumigatus fresenius* F-838 by Mizoue and co-workers of Taisho pharmaceutical company in 1985, is reported to induce the differentiation of leukemia in cultures and to inhibit the growth of certain Gram-positive bacteria and fungi.[11] Recently, Rovis and Orellana reported the synthesis of the spirobicyclic core of FD-838 via the asymmetric Stetter reaction.[12] Its total synthesis has not been accomplished, and its absolute configuration has been unknown, with its optical rotation being reported to be zero ($[\alpha]_D^{26}$ 0 (*c* 0.1, MeOH)).[10] As the fungus no longer produces FD-838, chemical synthesis is the only way to obtain this molecule. Despite the interesting biological properties, biological investigations cannot be performed because of lack of supply of FD-838.

Despite the structural similarity of FD-838, pseurotin A, synerazol, and azaspirene, the reported biological properties of these natural products are rather different, as described above. Systematic comparison of the biological properties of these natural products and their derivatives is highly desirable, and a sufficient quantity of not only the natural products but also several

* Corresponding author.
E-mail address: hayashi@ci.kagu.tus.ac.jp (Y. Hayashi).

0960-894X/$ - see front matter © 2009 Elsevier Ltd. All rights reserved.
doi:10.1016/j.bmcl.2009.03.154